The Abdus Salam
International Centre for Theoretical Physics

United Nations
Educational, Scientific and
Cultural Organization

IAEA
International Atomic Energy Agency

2060-44

Advanced School on Non-linear Dynamics and Earthquake Prediction

28 September - 10 October, 2009

Intermediate-term middle-range earthquake predictions in Italy: a review

A. Peresan
University of Trieste
DST/ICTP
Trieste
Italy

Available online at www.sciencedirect.com

SCIENCE DIRECT®

Earth-Science Reviews 69 (2005) 97–132

EARTH-SCIENCE REVIEWS

www.elsevier.com/locate/earscirev

Intermediate-term middle-range earthquake predictions in Italy: a review

A. Peresan[a,*], V. Kossobokov[b,c], L. Romashkova[b,c], G.F. Panza[a,c]

[a]*Department of Earth Sciences, University of Trieste, via E. Weiss 1, 34127 Trieste, Italy*
[b]*International Institute of Earthquake Prediction Theory and Mathematical Geophysics, Russian Academy of Sciences, Warshavskoe sh.79, kor. 2, Moscow 113556, Russia*
[c]*The Abdus Salam International Centre for Theoretical Physics, SAND Group ICTP, Miramare, 34100 Trieste, Italy*

Received 9 December 2003; accepted 7 July 2004

Abstract

The Italian territory has been the object of several studies devoted to the analysis of seismicity and to earthquake precursors' research. Although a number of observations have been claimed to precede large earthquakes, only few systematic studies have been carried out and almost no test of their performances is available up to now.

In this paper, we review the application to the Italian territory of two formally defined intermediate-term middle-range earthquake prediction algorithms, namely CN and M8S. The general methodology common to the two different algorithms makes use of general concepts of pattern recognition that permit to deal with multiple sets of seismic precursors, and allows for a systematic monitoring of seismicity, as well as for a widespread testing of the prediction performances.

Italy represents the only region of moderate seismic activity where the M8S and CN algorithms are applied simultaneously for routine monitoring. Significant efforts have been made to minimize the intrinsic space uncertainty of predictions and the subjectivity of the definition of the areas where precursors should be identified. Several experiments have been dedicated to assess the robustness of the methodology against the unavoidable uncertainties in the data. With these results acquired, starting in July 2003, an experiment was launched for the real-time test of M8S and CN predictions.

Keywords: Earthquake prediction; Pattern recognition; Prediction algorithms; Seismicity and seismotectonics; Italy

1. Introduction

The vulnerability of mankind to disasters induced by the growth and concentration of population, economy, radioactive, toxic and other dangerous materials and industries, has increased dramatically in the last few decades and keeps rising. The 1995

* Corresponding author. Tel.: +39 40 558 2129; fax: +39 40 558 2111.
E-mail address: anto@dst.units.it (A. Peresan).

0012-8252/$ - see front matter © 2004 Elsevier B.V. All rights reserved.
doi:10.1016/j.earscirev.2004.07.005

Kobe, Japan earthquake evidenced that the loss from a single seismic event already surpassed the level of US$100,000,000,000 (CAT-i Service, 2000). Surely, earthquakes are not the only source of risk; however, six of them are listed among the world's top 20 natural catastrophes in the last decade of the 20th century. These earthquakes were far from the largest, but generated 35% of total economic losses from natural disasters, ahead of floods (30%), windstorms (28%) and others (7%), as reported in CAT-i Service (2000). Earthquakes also cause the most fatalities. To effectively mitigate the damage from an earthquake, efforts must be shifted from the highly expensive post-disaster rescue and relief operations (prevalent in many countries) to cost-effective advance actions aimed at creating knowledge-based hazard-resilient public assets. Earthquake prediction, by providing basic knowledge of expected earthquake time and location, can be helpful in reorienting the current strategies toward increased earthquake preparedness. That is why earthquake prediction is widely recognized among the most challenging scientific problems, both due to its societal relevance and to the intrinsic complexity of the problem.

Can we predict earthquakes? The question remains a subject of numerous controversial discussions and debates (e.g. Geller et al., 1997; Wyss, 1997a; Nature Debates, 1999) but of a surprisingly small number of systematic studies. Although thousands of observations have been claimed to precede large earthquakes, there are almost no quantitative definitions of "precursors". Sir Charles Richter, despite his critical attitude to predicting earthquakes (his sentence "Only fools and charlatans predict earthquakes" is often cited in discussions on the subject), wrote a one-third of a page discussion (Richter, 1964) about a publication by Vladimir I. Keilis-Borok and Lydmila N. Malinovskaya (Keylis-Borok and Malinovskaya, 1964) that described observations of general increase in the seismic activity. He noted, in particular, "a creditable effort to convert this rather indefinite and elusive phenomenon into a precisely definable one", marked as important a confirmation of "the necessity of considering a very extensive region including the center of the approaching event", and outlined "difficulty and some arbitrariness, as the authors duly point out, in selecting the area which is to be included in each individual study". The methodology described in this paper did originate in the spirit of this early study at the time when the information database on earthquakes became large and complete enough to allow a meaningful systematic analysis of hypotheses about phenomena claimed precursory to large earthquakes (Sadovsky, 1986; Keilis-Borok and Soloviev, 2003). The methodology is based on general concepts of pattern recognition that automatically implies strict definitions and reproducible prediction results. The quantifiable uncertainty that remains is due to essential uncertainties in the data, which are therefore unavoidable.

The predictions arising from applications of the methodology of intermediate-term middle-range prediction (Sadovsky, 1986; Keilis-Borok and Soloviev, 2003 and references therein) were presented to the U.S. National Earthquake Prediction Evaluation Council (NEPEC) and NEPEC has recommended that the U.S. Geological Survey will undertake an extensive evaluation of this approach to the problem (Updike, 1989). The evaluation resulted in launching the experimental systematic prediction of the largest earthquakes worldwide (Healy et al., 1992) and, eventually, the outcome of the testing to date (Kossobokov et al., 1999b) permit to conclude the statistical validity and reliability of the methodology.

At about the time when the methodology (Sadovsky, 1986) was under evaluation at NEPEC, the Subcommission on Earthquake Prediction of the International Association of Seismology and Physics of the Earth's Interior (IASPEI) launched the Call for precursor nominees. The nominations of the intermediate-term middle-range earthquake prediction algorithms (Sadovsky, 1986) were excluded from the IASPEI list as being already submitted to NEPEC, although each of them did satisfy the Guidelines of the Call. In fact, the IASPEI validation criteria for precursor candidates are the following: (1) the observed anomaly should be related to some mechanism leading to earthquakes; (2) the anomaly should be simultaneously observed at more than one site or instrument; (3) the definition of the anomaly and of the rules for its association with subsequent earthquakes should be precise; (4) both anomaly and rules should be derived from an independent set of data, than the one for which the precursory anomaly is claimed. With reference to each of these requirements, the considered algorithms possess the following

features: (1) are based on empiricism guided by the concept of deterministic chaos; (2) give statistically significant results at a global scale; (3) are fully formalized published algorithms; (4) have been defined globally, using independent information from past seismicity to predict new strong earthquakes. As a result of the Call for precursor nominees, 31 candidates were included in the IASPEI list (Wyss, 1991). None of them were found to fully satisfy the Guidelines, mainly due to the eventual inability of authors to provide a precise definition of the observed phenomenon. The situation did not change much in the second round of evaluation (Wyss, 1997b): only five possible precursors, out of the 40 precursory observations submitted, seemed to deserve further study in the framework of earthquake prediction; nevertheless, none of them could be considered yet as a validated precursor.

The United States National Research Council, Panel on Earthquake Prediction of the Committee on Seismology suggested the following definition (Allen et al., 1976, page 7):

"An earthquake prediction must specify the expected magnitude range, the geographical area within which it will occur, and the time interval within which it will happen with sufficient precision so that the ultimate success or failure of the prediction can readily be judged. Only by careful recording and analysis of failures as well as successes can the eventual success of the total effort be evaluated and future directions charted. Moreover, scientists should also assign a confidence level to each prediction."

According to this definition, one can identify the prediction of an earthquake of a certain magnitude range by the duration of time interval and/or by the territorial specificity. Commonly, temporal classification loosely distinguishes long-term (tens of years), intermediate-term (years), short-term (tens of days), and immediate (days and less) predictions.

Following the common (but incorrect) perception that earthquake prediction means a 100% reliable short-term warning of hours, many investigators, besides longer term predictions, overlook spatial accuracies as well and concentrate their efforts on trying to predict the "exact" fault segment to rupture, like in the Parkfield earthquake prediction experiment (Bakun and Lindh, 1985). This is by far a more difficult task and it might be even an unsolvable problem. Being related to the rupture size, L, of the incipient earthquake, such prediction modes could be summarised in a classification that distinguishes, besides the "exact" location of a source zone, wider prediction ranges (Table 1).

Table 1
Classification of predictions

Temporal (in years)		Spatial (in units of the source zone size L)	
Long-term	about 10	Long-range	up to 100
Intermediate-term	about 1	Middle-range	5–10
Short-term	0.01–0.1	Narrow	2–3
Immediate	0.001	Exact	1

From the viewpoint of such a classification, the earthquake prediction problem might be approached by a hierarchical, step-by-step prediction technique, which accounts for multiscale escalation of seismic activity to the main rupture (Keilis-Borok, 1990), which starts with the term less zero-approximation, i.e. the recognition of the earthquake-prone zones without any information about the time of occurrence, for earthquakes from a number of magnitude ranges, then follows with the determination of long- and intermediate-term times and long- and middle-range areas of increased probability, and, finally, may come out with an exact short-term or immediate alert. The hierarchical nature of earthquakes suggests considering a hierarchical set of predictions, where the size of the events is given with an accuracy of about one unit of magnitude, i.e. one decimal order of the source area. In case of a magnitude range wider than one unit of magnitude, due to the Gutenberg–Richter (GR) relationship, the statistics of successes and failures is dominated by outcomes in predicting earthquakes at the lower limit of the range. Therefore, in practical application, it is preferable to define a set of magnitudes that identify target earthquakes, e.g. 8.0, 7.5, 7.0, etc. (Kossobokov et al., 1999a).

1.1. Why Italy?

The recent book by Keilis-Borok and Soloviev (2003) provides the state of the art at a global scale of the prediction methodology based on pattern recognition. This review paper, therefore, is focussed on their application to Italy, where, for the first time, two

different middle range algorithms, namely the M8S and CN algorithms (described in Section 2), are utilized simultaneously for the routine monitoring of rather moderate seismic activity.

In Italy, several studies have been devoted to earthquake precursor' research aimed, in particular, to investigate the premonitory features of seismic activity, during the last centuries (some historical information about early precursory observations can be found in Martinelli, 2000). Although a number of observations have been claimed to precede large earthquakes, these are frequently based on retrospective analysis and on single case studies. Only few systematic studies have been performed and practically no test in forward analysis has been carried out up to now.

A first successful attempt in forward prediction of earthquakes was done by Caputo (1983), based on the analysis of sequences of large earthquakes in Southern Italy; the prediction was confirmed by the occurrence of a moderately large event, which took place in May 1984 in the Abruzzo region (Caputo, 1988). Later on, an attempt to predict an earthquake in the Garfagnana region was done in 1985, based on the observation, still not formalized nor scientifically documented, of a potential foreshock. The area was evacuated, but the warning resulted to be a false alarm. The negative social impact of such an unsuccessful prediction called for a negative attitude to any prediction of earthquakes, which eventually discouraged further testing many precursors. In a paper following that event, Grandori et al. (1988) studied the foreshock–main shock correlation in three different regions of Italy (Garfagnana, Friuli and Irpinia) and found that short-term precursors based on potential foreshocks have a high probability to result in false alarms, an outcome quite similar to that obtained for Southern California (Jones, 1985). The same authors pointed out the advantages of prediction systems based on multiple independent precursors.

The univocal definition of the predictive rules and the possibility to test them against real observations represents the main shortcoming of the major part of the proposed precursors thus far (Wyss, 1991, 1997a,b). For example, the attempt to forecast the occurrence of large crustal events in Italy (Boschi et al., 1995b), by probability estimations within individual seismogenic zones (over time windows of 5, 20 and 100 years, respectively) cannot be regarded as earthquake prediction according to the definition by Allen et al. (1976). In fact, the ultimate success or failure cannot be judged without setting, in advance, the exact values of the probability cut-off that determines an alarm and the target magnitude range. This is a necessary decision required for an unambiguous definition of the alarm. Such forecast method is not based on the occurrence of precursors, but rather on the attempt to statistically describe the recurrence of large earthquakes within very narrow regions. Still, when checking the results provided by such an approach against observations (this is possible only for the first time window, as about 8 years have elapsed since the publication), it is possible to observe that no strong event occurred within the areas associated with the highest probabilities of occurrence within 5 years, while relatively large events (like the 1997 Umbria–Marche events) occurred in zones whose assigned probability was much lower.

A further example is provided by a middle-term seismic precursor that has been proposed, by retrospective analysis, for the large events ($M \geq 6.0$) which may occur in a given area of Southern Italy (Mantovani and Albarello, 1997). In this case, taking into account the "site-specificity" of the precursor and the long recurrence time of the large earthquakes within the given region, to check the significance of such predictions would require an unevenly long time.

The first attempt to search in the Italian seismicity for some formally defined premonitory patterns (i.e. "*swarms*" and "*bursts of aftershocks*"), that were already detected in other regions of the world and that could be eventually tested in forward predictions, was done by Caputo et al. (1977, 1983).

The effort to set up a systematic and testable analysis of seismicity, with the purpose of intermediate-term and middle-range earthquake prediction, started in Italy in 1990 (Keilis-Borok et al., 1990) with the first application of CN algorithm, which is based on a set of premonitory seismicity patterns (described in Section 2). During the initial stages of the experiment the basic problems related to the timely upgrading and the quality of the input data (i.e. completeness and homogeneity of the earthquake catalogue) were singled out. As it became clear that the originally available catalogue did contain a systematic error in magnitude determination (Peresan et al., 2000), the data routinely used for updating

predictions since 1998 is from the National Earthquake Information Centre (NEIC, 1990); a detailed description of the used catalogue is provided in Appendix A. Several tests have been performed to assess the robustness of the methodology against the data uncertainties (Peresan et al., 2000, 2002), and their results showed that significant systematic errors in magnitude could be spotted beforehand and, thus, do not compromise the diagnostic process. With these results acquired, predictions are routinely issued by CN algorithm, since January 1998, and by M8S algorithm, since January 2002. Starting July 2003, an experiment was launched, similar to the global one ongoing for M8 algorithm (Healy et al., 1992; Kossobokov et al., 1999b), but focussed on the Italian region and involving both CN and M8S algorithms. The goal of the experiment is to accumulate a collection of correct and wrong predictions (the latter include the false alarms and/or the failures to predict encountered in the test). Details about the experiment can be found at the web site: http://www.ictp.trieste.it/www_users/sand/prediction/prediction.htm. This, we believe, is the only way to evaluate a prediction algorithm and is essential for further development of the earthquake prediction methodology.

In this paper we provide a description of the methodology along with the scheme of data analysis and a detailed description of the applied algorithms (Section 2), then we review their application to the Italian territory (Sections 3 and 4). The obtained results and the possible practical use that can be made of such intermediate-term middle-range predictions are discussed.

2. Algorithms that use multiple precursors

Catalogues of earthquakes remain the most objective record of seismic activity on the Earth; that is why most of the studies concerning precursory phenomena, and therefore earthquake prediction, are based on the analysis of earthquake catalogues. Certain stability of the recording seismic activity is a necessary precondition of any search for precursory phenomena in earthquake sequences. It is of common knowledge that catalogues have errors, whose identification and elimination is desirable. The analysis of the frequency–magnitude graph of the catalogue for consistency, as well as special searches for duplicates and possible errors (Shebalin, 1992) are the essential part of every application of the methodology described below, which uses routine catalogues of earthquakes to express current dynamics of seismic areas (*areas of investigation*), derive *precursory seismicity patterns* at the approach of large earthquakes and make predictions based upon these reproducible determinations.

In agreement with the theory of non-linear dynamical systems we expect detectable variations of observables at the approach to a singularity (critical point, catastrophe). Moreover, the discrete and chaotic nature of seismic processes suggests describing each area of investigation with robust trailing averages of the parameters used to quantify specific patterns of seismic activity, the so-called *traits*. The differences of an informative trait values in periods associated with extreme events and outside of them provide the basis for search of *precursory seismicity patterns* (that is, the typical values assumed by the considered set of traits during the periods of time preceding the large earthquakes). This search eventually determines *criteria*, i.e. permits to delimit a specific volume in the space of traits values that characterise so-called "*Time of Increased Probability*" (TIP), from the time when a large earthquake should not be expected. One or several informative traits could be used for prediction. Moreover, a combination of traits may be informative for prediction if some or even all of them show unsatisfactory performance when applied separately.

To establish the precursory nature of a seismicity pattern, one needs ultimate testing in an experimental prediction of earthquakes in the real-time mode. For this purpose, one must design a prediction algorithm that implements criteria and recognizes at a given time those areas of investigation, where strong earthquakes should be expected. The accumulated statistics of successes and failures, on one hand, and the proportion of areas of alarm, on the other, provide information for the conclusion whether or not the seismicity pattern is precursory.

Obviously, this general scheme is open for inclusion of many traits and other data, not necessarily seismological.

The algorithms applied in this paper are based on the simultaneous quantitative analysis of a set of *precursory seismicity patterns* (Keilis-Borok and

Rotwain, 1990; Keilis-Borok and Kossobokov, 1990). The following variations have been observed in the seismicity in a time interval of 2–3 years before strong earthquakes (intermediate-term precursors):

- Increase of the seismic activity;
- Strong time fluctuations of the seismic activity;
- Clustering of the aftershocks in space and time;
- Long-range interactions;
- Increase of the space clustering of seismic sources.

These symptoms may be interpreted as an increased response of the lithosphere to the tectonic stress and are symptomatic of the critical state of the system before the occurrence of a strong earthquake; such a response is common to many other non-linear systems prior to a catastrophic event (Keilis-Borok, 1996).

One of the most relevant properties of these precursory phenomena is the *similarity*; in robust definition, i.e. after appropriate averaging, the seismicity patterns to be used for predictions appear to be the same in a wide variety of tectonic environments, at least for magnitudes $M \geq 4.5$ (Keilis-Borok and Soloviev, 2003). This similarity is limited and disappears, leaving place to the regional variations of the premonitory features, when the phenomena are not averaged in space and time. The similarity of precursors is essential in order to collect an amount of observations sufficient for statistical interference of their significance in realistic time. In fact, even if on global scale strong earthquakes are not infrequent, within any region small enough to be considered for prediction purposes, they are rare events, characterised by long inter-event times.

An essential step, when analysing premonitory seismicity patterns, consists of the definition of the area where precursors have to be searched, the *area of investigation*, which is strictly interrelated with the size of the events to be predicted. For natural reasons, the size of the area should increase with the rupture size $L=L(M_0)$, where M_0 is the magnitude threshold selecting the target earthquakes. In particular, for the application of the methodology considered in this paper, it has been found empirically that the linear dimensions of the monitored area must be greater or equal to $5L$–$10L$. In fact, the preparation of a large earthquake may involve a system of faults rather than a single fault, hence non-local precursors, including migrations of seismicity, may reflect some underlying large-scale processes, which cannot be explained by the simple post-seismic stress redistribution in an elastic medium, but are typical in self-organised critical systems. This evidence is supported by the independent observation of Bowman et al. (1998), who found that the size of the region, where accelerated seismicity can be observed, scales with the magnitude and is much greater than that predicted by simple elasto-dynamic interactions. Consequently, the seismic precursors must be searched within the regions having linear dimensions of several hundred kilometers, in order to take into account possible long-range correlations. Despite their shape and position having a real objective significance, there is still obvious difficulty of arbitrariness in selecting areas of investigation.

The condition imposing that the size of the area of investigation is much larger (5–10 times) than the rupture size of an event with magnitude M_0 is especially relevant in view of the Multiscale Seismicity (MS) model (Molchan et al., 1997). In fact according to the MS model, the Gutenberg–Richter (GR) law describes adequately only the ensemble of earthquakes that are geometrically small with respect to the dimensions of the analysed region. In the original global formulation by Gutenberg and Richter (1956), all the earthquakes could be approximated to points, since even the sources of the largest events are negligible with respect to the Earth's size; therefore the linearity of the GR was holding up to the largest magnitudes. On the contrary, when focussing on a delimited region, the point approximation could no longer be valid; as an example, an event with $M=7$, whose surface rupture length can be estimated at around 50 km (Wells and Coppersmith, 1994) can be considered point-like only within a region of linear dimensions larger than 500 km. In agreement with the MS model, when seismicity is analysed over relatively small regions, the frequency–magnitude relation is linear (Self-Organised Criticality, SOC) only up to a certain magnitude, while for the larger events it usually exhibits an upward bend (Characteristic Earthquake, CE). Specifically, within the areas delimited for prediction purposes, the number of earthquakes with $M>M_0$ (whose source size becomes comparable with the region size) generally exceed the

estimation based on the extrapolation of the GR law (SOC) and hence they can be considered abnormally strong (CE) within the given region. At the same time the MS model guarantees the self-similarity condition for the small and moderate events ($M<M_0$), considered for the analysis of the premonitory patterns, and hence the long-linearity of the frequency–magnitude relation in the magnitude range of interest. In such a way, the algorithms make use of the information carried by small and moderate earthquakes, statistically characterised by the GR law and its generalizations (Kossobokov and Mazhkenov, 1994; Bak et al., 2002; Corral, 2003), to predict the strong earthquakes, which are anomalous and often arbitrarily interpreted as characteristic events inside the regions delimited for prediction purposes.

The dependence of the linearity of the GR relation on the dimensions of the investigated area is illustrated considering different regions of the World (Fig. 1) as well as the Italian territory (Fig. 2). Fig. 1 displays real seismic data from the eastern hemisphere and southern California that were used (Kossobokov and Mazhkenov, 1994) along with other examples to justify generalizing the GR law in the form:

$$\log_{10}N = A + B(5 - M) + C\log_{10}L \qquad (1)$$

where $N=N(M, L)$ is the expected annual number of earthquakes with magnitude larger than M in an area of linear dimension L; A and B are similar to the coefficients of the GR relation, while C estimates the fractal dimension of the earthquake-prone faults. Such a Unified Scaling Law for Earthquakes states that the

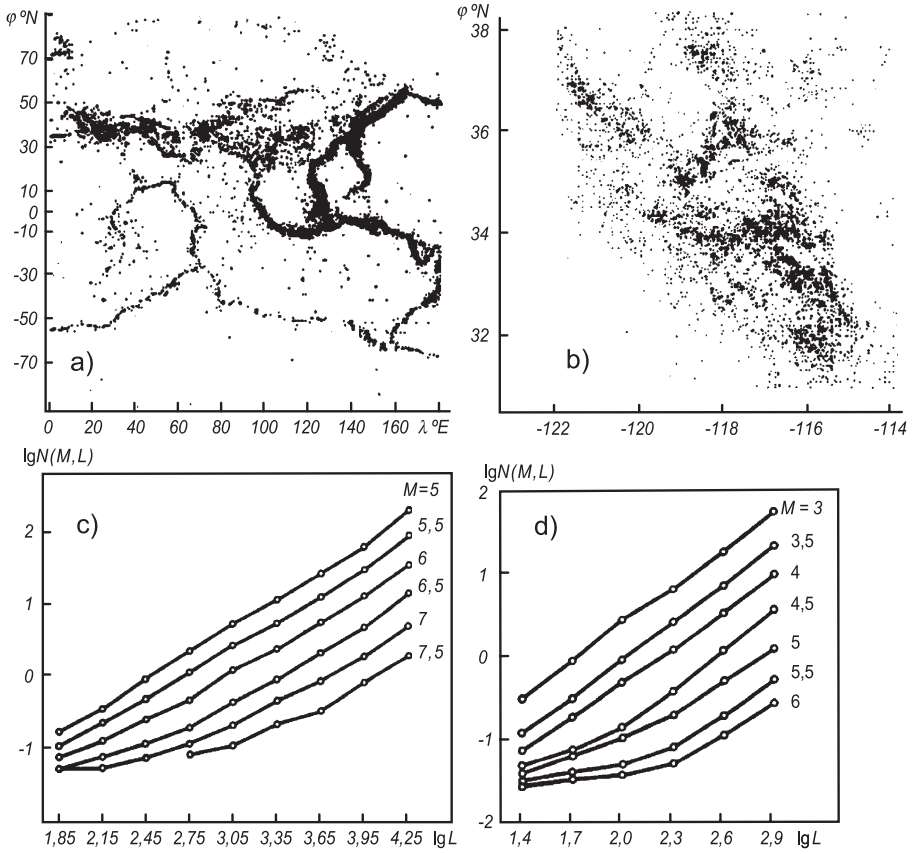

Fig. 1. Spatial distributions of epicenters in (a) Eastern Hemisphere (1964–1985) and (b) Southern California (1949–1985) along with the corresponding log$N(M, L)$ graphs (c,d) from Kossobokov and Mazhkenov (1994), which suggest that the empirical counts fitting a plane in (log$N$, M, log$L$)–space.

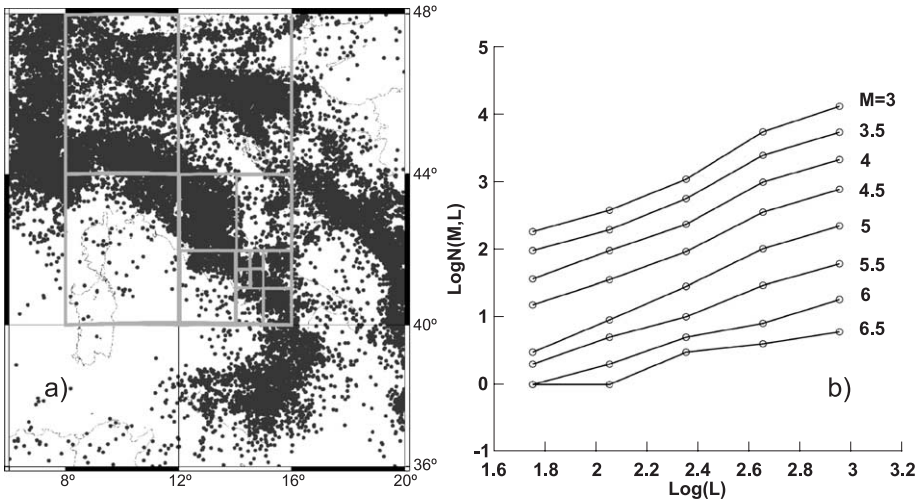

Fig. 2. Spatial distributions of epicenters in the Italian region and areas of scaling size, from L=8° to L=0.5°, considered for events counting (a) and plot of the cumulative number of events log$N(M, L)$ versus the size log(L) of the considered area (b). All the events reported in the UCI2001 catalogue (described in Appendix B) during the period 1900–2002 are considered.

distribution of rates or waiting times between earthquakes depends only on the local value of the control parameter $10^{-BM}\ L^{C}$, which represents the average number of earthquakes per unit time, with magnitude greater than M occurring in the area size $L\times L$. The counts of N on the original seismic data (Fig. 1c,d) for smaller magnitude ranges demonstrate a clear linearity in bi-logarithmic scale over 8, at least, doublings of the area dimension L. The GR relation is observed as near-equal spacing between the lines corresponding to different magnitude ranges; with magnitude increase the linearity truncates with decreasing dimension of area, as soon as the recurrence of such earthquakes in it compares to the time span of the catalogue used. The Italian data (Fig. 2) confirms the Unified Scaling Law for Earthquakes for a time period of a century. The local variability of seismic regime and its deviations from steady stable behaviour is the key to the gates of earthquake prediction.

The general scheme of the analysis for the considered methodology (Sadovsky, 1986), based on *multiple premonitory patterns*, is as follows. We first define the *strong earthquake*, as the target one, by the condition that is magnitude $M\geq M_0$. In most cases, the choice of M_0 is predetermined by the recurrence time of strong earthquakes in the territory considered. As a second step, we define the *areas of investigation*, that overlay the territory under study and whose size depend on M_0.

Each area of investigation at a given time t is an *object of pattern recognition*, described by selected parameters of the recent seismic dynamics. The sequence of earthquakes which occur within an area of investigation, as defined by their origin times, locations and magnitudes, is indicated as *seismic flow*. The features of the earthquake sequence within the given area are quantified by means of several empirical *functions of the seismic flow* (Gabrielov et al., 1986); these functions of time, t, are estimated considering the sequence of main shocks within trailing time windows of different length with common end in t. The robust trailing averages of such parameters, the so-called *traits*, are then analysed in order to single out the most informative ones, i.e. those that change sensibly before the occurrence of large events. This permits to define the *precursory seismicity pattern*, a set of characteristic traits which distinguish the periods of time preceding the large earthquakes ("dangerous" periods, D) from those when no strong event has occurred ("non-dangerous" periods, N). This set of typical traits is then used as criteria that recognize whether a given *object*, associated to the area of investigation at the instant t, belongs to a *Time of Increased Probability* (TIP), i.e. to a period when a large earthquake should be expected.

In the methodology applied in this paper, the identification of the set of characteristic traits, known

as *the learning phase* of the pattern recognition procedure, has been performed only during the stage of the algorithms design, based on the careful analysis of seismicity in a well-documented region (e.g. the California–Nevada region for CN algorithm). The learning stage is not repeated when applying the algorithms to other areas, thus assuming that the seismic premonitory patterns are the same in different regions worldwide. The assumption of similarity of symptoms is essential to permit their testing against observations and significantly reduces the number of degrees of freedom of the procedure.

To account for the diverse size and level of seismic activity in the different areas of investigation, without the necessity to adjust the parameters of the algorithms, the functions of the seismic flow are *normalized* by thresholds in magnitude, which are selected on the basis of the average return period of events observed during the *thresholds setting period*. The functions are discretised into small, medium and large values, according to the level of seismic activity in the considered area, and the thresholds for discretisation are selected by the retrospective analysis of seismicity within the thresholds setting period. The thresholds setting period must correspond to an interval of time long enough to provide a representative sample of the seismic activity within the considered area of investigation, including periods of quiescence as well as periods of high activity (Keilis-Borok and Rotwain, 1990). The discretisation of the functions and the robust definition of the running averages, may cause some loss of information but make the algorithms robust with respect to fluctuations in the data, so that a reasonable variation of the parameters does not affect the predictions (Peresan et al., 2002). At the same time, the discrete character of the seismic data and the strict usage of the prefixed thresholds result in the discreteness of the alarms (i.e. yes/no alarm).

It is worth noticing that the learning phase, which involves the definition of the functions of the seismic flow and the selection of the characteristic traits, is performed only once, during the stage of design of the algorithms. The thresholds setting stage, instead, is performed each time the algorithm is applied to a different region, in order to select the magnitude thresholds for the computation of functions, as well as the thresholds for their discretisation, according to its level of seismic activity.

Based on the recognition of a given set of characteristic traits, the algorithm establishes whether the object, associated to the area of investigation at the time t, belongs to the class of objects that precede the strong earthquakes and eventually declares a TIP. When a strong event occurs during a TIP, then it is indicated as a *successful prediction*; otherwise, it is referred to as *failure to predict*. If no strong earthquake occurs during a declared TIP, then the TIP is called a *false alarm*. According to Molchan (1990), the results of a prediction for a given area of investigation can be characterised by two types of errors. The first one is the percentage η of failure to predict; $\eta=F/N$, where F is the number of failures to predict and N is the number of events to be predicted. The second one is the percentage τ of the total duration of alarms: $\tau=A/T$, where A is the total duration of alarms and T is the length of the whole time interval considered. According to Molchan (1990, 1996), the quality of the predictions can be quantified by the sum of the errors; $\Omega=\eta+\tau$; since the random prediction gives $\Omega=1$ (Molchan, 1990), one can roughly estimate the quality of prediction by the deviation of Ω from unity.

Despite the considered algorithms being fully formalized, the reliability of results obviously depends on the proper performance of the different steps of the analysis and on the quality of the input data. Therefore, some guidance may be necessary for a correct understanding of the methodology, as well as for a careful checking of the space–time completeness and homogeneity of the input catalogue, when applying the algorithms for earthquake prediction purposes.

2.1. Description of CN algorithm

The algorithm CN (Gabrielov et al., 1986; Keilis-Borok and Rotwain, 1990) is an intermediate-term middle-range prediction algorithm which has been designed by the retrospective analysis of the seismicity patterns preceding the large earthquakes in the California–Nevada region (hence its name). CN is structured according to a pattern recognition scheme (Keilis-Borok and Soloviev, 2003 and references therein) to allow a diagnosis of TIPs for the events with magnitude above a fixed threshold M_0, based on a given set of *multiple premonitory patterns*.

The threshold M_0 for the selection of the events to be predicted is defined by the following three simultaneous conditions: (1) the average return period of the earthquakes with $M \geq M_0$, occurred inside the area of investigation, is approximately 6–7 years; (2) M_0 is selected as close as possible to a minimum in the histogram of the number of events versus magnitude, since this guarantees a certain stability of the results (Molchan et al., 1990); (3) in the magnitude range considered, the catalogue is sufficiently complete for the estimation of the functions, i.e. $M_0 - \Delta M \geq M_c$, where M_c is the completeness threshold of the considered catalogue and $\Delta M \cong 3$.

The *area of investigation* for CN application is selected taking into account the spatial distribution of seismicity and the geometry of fault systems and must satisfy three general rules: (a) its linear dimensions must be not lower than $5L$–$10L$, where $L=L(M_0)$ is the rupture size of the target earthquake (estimated for example, using the empirical relation proposed by Wells and Coppersmith, 1994); (b) on the average, at least three events with magnitude over the completeness threshold should occur inside the area of investigation each year; (c) the border of the area must correspond, as much as possible, to minima in the seismicity. This indicates that the detection level controls, to some extent, the time–space uncertainty of prediction (Keilis-Borok, 1996) and then the possibility to reduce the spatial uncertainty is limited by the difficulty to keep a high level of detection, due to unavoidable logistic problems.

As discussed in Section 2, condition (a), together with the three conditions defining M_0, implies that in any monitored area of investigation, CN makes use of the information given by small and moderate earthquakes, having quite a good statistic (i.e. following the GR law), to predict the stronger earthquakes, which are anomalous events (i.e. do not follow GR law) for the same area.

The flow of the earthquakes is represented, at each time, t, by a vector $P(t)=(p_1(t),\ldots p_m(t))$ formed by the values $p_i(t)$ of the different functions that define the algorithm CN, evaluated within trailing time windows with common end in t. The functions estimated by CN are the following; $N_1(t)$, $N_3(t)$, $K(t)$, $G(t)$, $\Sigma(t)$, $S_{max}(t)$, $Z_{max}(t)$, $q(t)$, $B(t)$. These functions evaluate the variations in seismic activity, seismic quiescence, space–time clustering of the seismic activity and spatial concentration of the events. Specifically, the function G depicts the share of relatively higher magnitudes in the earthquakes sequence; K and q describe the variations of the sequence in time and the quiescence, respectively. The functions N_1 and N_3 are used to describe the level of seismic activity, while the function B, which is based on aftershocks counting, is a measure of the space and time clustering of earthquakes within the region. The value of Σ is proportional to the seismic energy released (*source energy*), Σ; the maximal values of "source area and diameter", S_{max}, are proportional to the average area of the source; finally Z_{max} represents the linear concentration of the main shocks. A detailed description of the functions is given in Appendix A. The functions of the seismic flow are evaluated on the sequences of the main shocks which occurred in the area of investigation, the aftershock being identified according to the *window method* proposed by Keilis-Borok et al. (1980). The operating magnitude is selected from the available ones following a specified *priority order* (i.e. an ordered list of preferred magnitudes), which is defined taking into account the properties of the different magnitude estimations in the given catalogue. This allows us to consider the magnitude that appears to be the most reliable, whenever it is provided, and at the same time, permits to use all of the events having an assigned magnitude. Usually, only shallow events are considered for CN application (Keilis-Borok and Rotwain, 1990; Costa et al., 1996).

Three different classes of time intervals are identified along the time axis; D (Dangerous), N (Non-dangerous) and X (Undetermined). The D intervals extend for 2 years before each strong event. The intervals X extend for 3 years after each strong event; if a strong earthquake occurs within an interval X, then it is classified as D interval. The remaining time intervals are classified as N intervals. The subdivision of the time axis is used at the stage of pattern recognition in order to select the objects necessary for the learning (learning set). The time intervals X are excluded from this stage of the analysis. Following the pattern recognition procedure (Gelfand et al., 1976), values of the functions are coarsely discretised into "small", "medium" and "large" values, by defining the thresholds on the basis 33- and 66-percentile (i.e. thresholds corresponding to

33% and 66% of the encountered values). Then the characteristic traits (described by single functions or by combinations of different functions), which are typical for intervals D and *N*, are selected. The features D are defined by the condition that they are observed in most of the cases during the intervals D, and just in a few cases during the intervals N; the features N are defined by the opposite condition. Each feature corresponds to a discretised value of the function or to a combination of such values for two or three functions.

At the stage of voting, every time t, either belonging or not to the learning set, is evaluated regardless of its position with respect to the occurrence time of a strong shock (i.e. without any a priori classification). A TIP for an earthquake with $M \geq M_0$ is declared at the time t and for 1 year if:

1. the difference $\Delta(t)$ between the number of the features D and N, at the time t, is greater or equal to a given constant $\bar{\Delta}$:

$$\Delta(t) = n_{\mathrm{D}}(t) - n_{\mathrm{N}}(t) \geq \bar{\Delta} \qquad (2)$$

   where usually $\bar{\Delta}$=5.
2. the total source area $\sigma(t)$ for the earthquakes which occurred during a period of 3 years before time t, is lower than constant $\bar{\Sigma}$:

$$\sigma(t) = 10^{-\beta(M_0-\alpha)}\Sigma\left(t|\underline{M}, s, \alpha, \beta\right) < \bar{\Sigma} \qquad (3)$$

where $\bar{\Sigma}$=4.9 is the standard value defined for the California–Nevada region.

These two conditions mean that at the time t the D features are predominant and that the seismic energy already released, during the past 3 years, is not high. Consecutive TIPs may overlap and hence an alarm period may exceed 1 year.

The normalization of the functions, which permits to apply CN areas of investigation with a different level seismic activity without any ad hoc adjustment of the parameters, is achieved by means of the "equalization" of the seismic flow; three thresholds of magnitude, $m_1 \leq m_2 \leq m_3$, are selected in such a way that:

$$\bar{\mathrm{N}}(M \geq m_1) \geq a \qquad \bar{\mathrm{N}}(M \geq m_2) \geq b \qquad \bar{\mathrm{N}}(M \geq m_3) \geq c \qquad (4)$$

Table 2
Standard time and magnitude windows for CN functions (see Section 2.1)

	N_1	N_3	K	G	Σ	S_{max}	Z_{max}	q	B
s	3	3	2	3	3	3	3	6	3
$\underline{M}$	M_3	m_2	m_2	m_2	m_1	m_1	m_1	m_2	–
$\overline{M}$	–	–	–	–	M_0-1	M_0-1	M_0-1	–	–

where $\bar{N}$ is the yearly average number of events which occurred inside the selected area of investigation, and a=3.0, b=1.4 and c=0.4 are given constants, equal for all the areas worldwide. The magnitude range $\underline{M} \leq M \leq \overline{M}$ considered to estimate the different functions is thus defined, for each area, using m_1, m_2 and m_3. The standard length of the time window s (in years) and the magnitude thresholds, $\underline{M}$ and $\overline{M}$, used for each of the CN function are given in Table 2.

Within each area of investigation we therefore consider the earthquakes with the long-term average annual number $\tilde{N}=\bar{N}=M \geq m_1=3$ (main shocks). Compared with the standard value $\tilde{N}$=20, used in algorithm M8, this implies a higher magnitude cut-off $M_{\min}$ and, therefore, more loose requirement to the catalogue.

The standard application of the algorithm to a given region does not require to repeat the whole pattern recognition procedure, but just to define the area of investigation and the threshold M_0 for the selection of the events to be predicted. The magnitude thresholds for the normalization of functions and the thresholds for their discretisation are then automatically adjusted on the basis of the retrospective analysis of seismicity during the *thresholds setting period*. This stage of the analysis has been often erroneously indicated as the *learning stage*, to distinguish it from the stage of voting (i.e. recognition of the time intervals); nevertheless, it is necessary to bear in mind that, in all the worldwide standard applications the premonitory patterns searched in the seismic flow are those selected for the California–Nevada region, when the prototype of CN (Gabrielov et al., 1986) was developed.

2.2. Description of M8 algorithm

2.2.1. The standard M8 algorithm

This intermediate-term middle-range earthquake prediction method was designed by the retrospective analysis of the dynamics in seismicity preceding the

greatest (magnitude 8.0 or more) earthquakes worldwide, hence its name. Its prototype (Keilis-Borok and Kossobokov, 1984; Kossobokov, 1986) and the original version (Keilis-Borok and Kossobokov, 1987) were tested retrospectively in the vicinities of 143 points, out of which 132 are recorded epicenters of earthquakes of magnitude 8.0 or greater from 1857 to 1983. In 1992, an experiment was launched aimed at a real-time intermediate-term middle-range earthquake prediction at a global scale. The global test of the algorithm M8 (Healy et al., 1992) aimed at the prediction of the largest earthquakes (defined by M_0=7.5 and M_0=8.0) was carried out routinely (Kossobokov et al., 1999b) in real-time for more than 10 years now (a complete record of predictions from 1985 to 2003 can be viewed at http://mitp.ru/predictions.html).

M8 is aimed at the prediction of earthquakes with magnitude M_0 and above. If the data are sufficiently complete, we distinguish a number of intervals $M_0 \le M < M_0 + \Delta M$ (indicated hereinafter as M_0+), considering values of M_0 with an increment of 0.5, unless actual distribution of earthquake size suggests a natural cut-off magnitude that determines characteristic earthquakes at different levels of earthquake hierarchy. The choice of ΔM from 0.5 up to 1.0 seems rather reasonable with respect to the actual accuracy of magnitude determination, as well as with respect to the earthquake size scaling, i.e. to the Gutenberg–Richter relationship.

Overlapping circles with the diameter $D(M_0)$ scan the seismic region under study. Within each circle, the sequence of earthquakes is considered with aftershocks removed, $\{t_i, m_i, h_i, b_i(e)\}$, i=1, 2 … Here t_i is the origin time, $t_i \le t_{i+1}$; m_i is the magnitude, h_i is the focal depth, and $b_i(e)$ is the number of aftershocks with magnitude $M \ge M_{\text{aft}}$ that occurred during the first e days. The sequence is normalized by the lower magnitude cutoff $\underline{M} = M_{\min}(\tilde{N})$, $\tilde{N}$ being a standard value of the average annual number of earthquakes in the sequence. Naturally, the magnitude scale we use should reflect the size of the earthquake sources. Accordingly, M_S (magnitude from surface waves) is usually taken for larger events while m_b (magnitude from body waves) is used for smaller ones, for which M_S determinations are not available. For many catalogues, this choice is equivalent to considering the maximum reported magnitude, e.g. we do so when using the National Earthquake Information Center/U.S. Geological Survey Global Hypocenters' Data Base (GHDB, 1989).

The features of the seismic sequence are quantified by computing several running averages (functions of the seismic flow) for the sequence, in the trailing time window $(t-s,t)$ and magnitude range $M_0 > M_i \ge \underline{M}$. They include different measures of intensity in the earthquake flow, its deviation from the long-term trend, and clustering of earthquakes. The functions of the seismic flow evaluated by the algorithm M8 include: $N(t)$, $L(t)$, $Z(t)$ and $B(t)$. The detailed description of the functions is given in Appendix A. Each of the functions N, L, Z is calculated twice, with a different magnitude cutoff $\underline{M} = M_{\min}(\tilde{N})$, for $\tilde{N}$=20 and $\tilde{N}$=10, respectively. As a result, the earthquake sequence is represented by a robust averaged description defined by seven functions: N, L, Z (twice each), and B. "Very large" values are identified for each function using the condition that they exceed Q percentiles (i.e. they are higher than Q percent of the encountered values).

A TIP is declared for 5 years, when at least six out of seven functions, including B, become "very large" within a narrow time window $(t-u, t)$. To stabilize the prediction, this criterion is required for two consecutive moments, t and t+0.5 years. When performing a forward application of the algorithm, the alarm may terminate before 5 years or may extend beyond it, in case after the updating the alarm conditions are no longer satisfied.

The following standard values of the parameters indicated above are fixed a priori in the algorithm M8: $D(M_0)=\{\exp(M_0-5.6)+1\}^0$ in degrees of meridian (this is 384, 560, 854 and 1333 km for M_0=6.5, 7.0, 7.5 and 8, respectively), s=6 years, s'=1 year, g=0.5, p=2, q=0.2, u=3 years (see the detailed description of the functions in Appendix A), and Q=75% for B and 90% for the other six functions. The quantity 5.6 in the relation defining $D(M_0)$ is the normalizing value that makes $D(M_0=8.0)=12^\circ$ in degrees of the Earth meridian (Keilis-Borok and Kossobokov, 1987). The dimension of the areas of investigation considered by M8 are set proportional to the linear dimensions of the target earthquakes (Dobrovolsky et al., 1979) and are independently confirmed by Bowman et al. (1998), who claimed that the size of the critical region of accelerated energy release scales with the magnitude of the impending event according to $\log_{10}R \sim 0.44$ M.

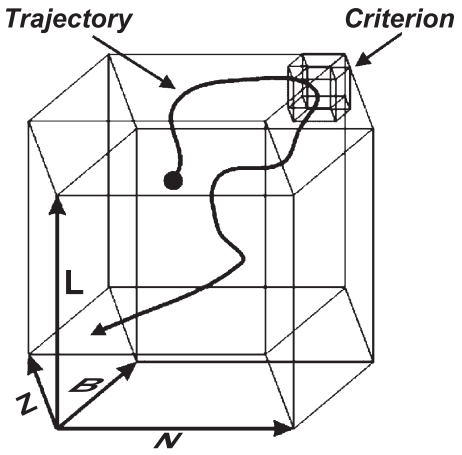

Fig. 3. The trajectory in the phase space (N, L, Z, B volume) describing the time dependent behaviour of an area of investigation. A criterion is a part of the phase space so that an entry of the trajectory into it indicates abnormal behaviour of the system. The M8 algorithm determines a TIP after the parameters of description—N, L, Z, B—show up extremely large values, i.e. after the trajectory enters the M8 algorithm criterion, smaller 4D-volume of the top values of parameters.

Qualitatively, the algorithm M8 uses a rather traditional description of a dynamical system adding to a common phase space of rate (N) and rate differential (L), a dimensionless concentration (Z) and a characteristic measure of clustering (B). The algorithm recognizes the *criterion* (Fig. 3) defined by extreme values of the phase space coordinates, as a vicinity of the system singularity. When a trajectory enters the criterion, the probability of an extreme event increases to the level sufficient for its effective prevision. The choice of the M8 criterion determines a specific intermediate-term rise, *inverse cascade* (Gabrielov et al., 2000), of seismic activity at the middle-range distance.

2.2.2. The spatially stabilized scheme: the M8S algorithm

In the standard application of the M8 algorithm, the circles of investigation (CI's) are placed along the line of maximal concentration of seismic epicenters, in order to cover all seismic-prone territory, of the region considered, with approximately three-times-overlap. This general rule was introduced at the time of low-speed computers to decrease the number of CI's, which also makes the results more transparent for independent testing (the original settings for the M8 testing in the Circum-Pacific fit one floppy disk and would run on IBM XT machine). The sparse location of CI's gives a rather wide freedom in the choice for each of the appointed circles. The problem of the prediction stability with respect to the positioning of CI's remained open until recently, although Bernard Minster and Nadia Williams were approaching the issue in their independent assessment (Minster and Williams, 1992, 1996), where they suggested essentially a new prediction algorithm based on M8 code. For an application in regions of moderate and low seismic activity, the issue of stability is crucial, in particular due to the extremely small samples of data available for determination of the alarm state of a CI. Therefore, the new scheme of the spatially stabilized M8, named M8S algorithm, was originally designed on the basis of the M8 application in Italy, which is a region of moderate seismic activity (Kossobokov et al., 2002). M8S depends less on the positioning of a particular circle and stabilizes the declaration of alarms. A brief description of the new scheme follows. Let us consider the territory covered by the data of a given catalogue and let us exclude the band of about $0.5R$–$1.0R$ near its boundary, where R is the radius of CI's. The territory is scanned with a set of small circles (ci) of radius r distributed over a fine grid, with a step s. All local seismically active places are identified as the grid points where the average annual rate of seismic activity a, in the small circle ci, is above a certain threshold. The grid points, where the data is insufficient for the application of M8 algorithm in the CI's centered on them, are excluded from the analysis and then the isolated grid points and pairs are removed. M8 algorithm is, therefore, applied to the CI's centered on each of the remaining grid points. The last step is the removal of the alarm circles centered on the grid points that do not satisfy the following clustering condition: the overwhelming majority n of the CI's, centered on the neighbouring grid points that remain in the analysis, are in state of alarm.

Thus, we first apply the M8 algorithm in the CI's whose centers are defined automatically from the distribution of earthquakes, and then disregard as sporadic some alarms that are not confirmed by alarms in the neighbouring circles.

There are some features of the M8S algorithm that distinguish it from the standard M8. The standard

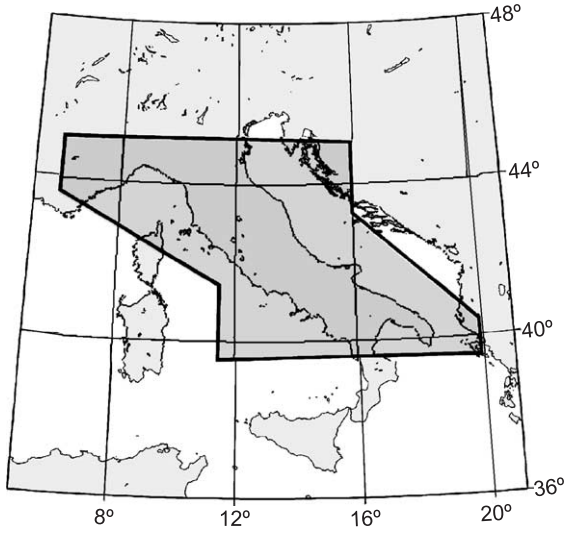

Fig. 4. Regionalization defined for the application of CN to the Italian territory by Keilis-Borok et al. (1990).

applications of M8 use a predefined number of circles of investigation during all periods of analysis. Due to the certain gradual increase of completeness of the catalogue, with M8S we operate with a changing number of CI's and, as a consequence, a changing area of the prediction territory. However, the presence of alarm at any particular point, for instance in a city, is easy to trace. At the same time, the improvement in the methodology makes the presence of an alarm much more reliable.

3. Algorithm CN in Italy

3.1. Choice of the areas of the regionalization

The algorithm CN was applied to the Italian territory for the first time in 1990 (Keilis-Borok et al., 1990), considering an area delimited on the basis of the completeness of the catalogue available at that time (see Appendix B). The necessary completeness for CN application is, starting from 1950, for latitudes between 39.5°N and 45.0°N and this led to the definition of the area of investigation shown in Fig. 4. The operating magnitude $M=M_{\text{priority}}$ considered by CN (simply indicated as M in this section), is selected according to the priority rule described in Appendix B. The threshold for the selection of the strong events, fixed to be M_0=5.6, corresponds to an average return period of about 6 years during the threshold setting period (1954–1986). The results obtained in the retrospective analysis are the following: four out of five strong events were preceded by TIPs, occupying about 26% of the total time, while there were three false alarms and one failure to predict.

A subsequent study by Costa et al. (1995) shows that seismological and tectonic arguments permit to narrow the area of investigation, leading at the same time to a reduction of failures to predict and of TIPs, and to increase the stability of the results with respect to the choice of the free parameters of the algorithm. Specifically, the analysis of the sequences of earthquakes inducing the activation of TIPs, permitted to observe that the events in the Gargano zone and near Ancona occurred only before false alarms, suggesting that such events might be independent from the seismicity in the Apennines. Hence, the area for CN application in Central Italy was narrowed to include only the high seismicity zones along the Apennines (Fig. 5). The retrospective diagnosis of TIPs, for events with magnitude larger than M_0=5.6, was performed using both the ENEL+ING+CSEM catalogue (Keilis-Borok et al., 1990) and the PFGING (Costa et al., 1995) catalogue, as described in Appendix B. The outcomes of these tests showed that all the strong events, included in the area of

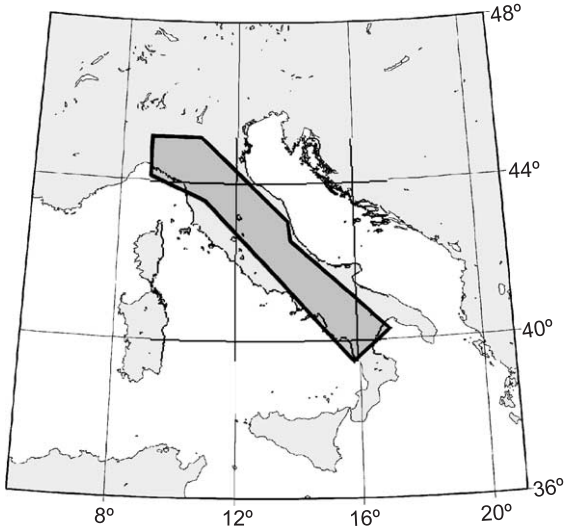

Fig. 5. Regionalization proposed for the Central Italy by Costa et al. (1995).

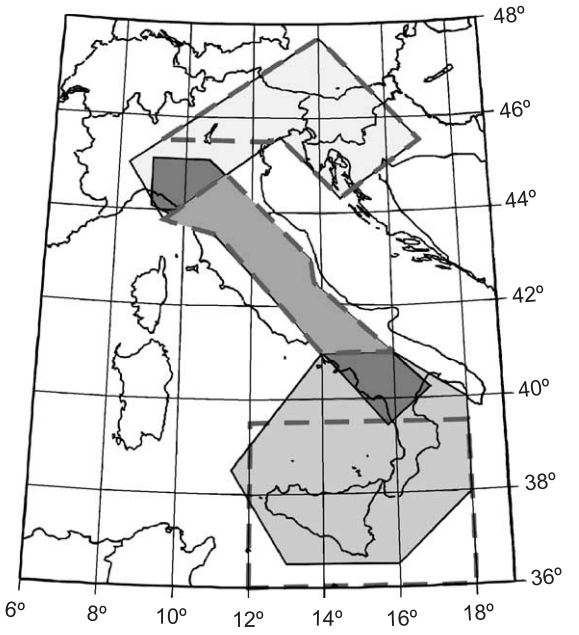

Fig. 6. Regionalization proposed by Costa et al. (1996). The areas of investigation which include the intersection domains (Area 1) are delimited by a continuous thin line (grey shadowed areas), while the areas excluding intersections (Area 2) are delimited by a thick dashed line.

investigation displayed in Fig. 5, could be predicted by considering an area which is about 15% of that proposed by Keilis-Borok et al. (1990). Moreover, the use of the PFGING catalogue allowed for a further reduction of the time uncertainty of prediction.

Later on, taking into account both the seismotectonic model (Scandone et al., 1990) and the spatial distribution of epicenters, the application of CN algorithm has been extended to the whole Italian territory (Costa et al., 1996), divided into three main areas, indicated as Northern, Central and Southern regions. The three selected areas of investigation are characterised by a predominant seismogenic behaviour and by a different level of seismic activity; for each of them two possible variants were considered, including (Area 1) or excluding (Area 2) the intersection domains (Fig. 6). One of the areas considered for Central Italy coincides with that defined by Costa et al. (1995). The Italian catalogue used for the analysis is basically the PFGING. The application of CN to the Northern region, however, required to integrate the catalogue with the local ALPOR and the global NEIC data (as described in Appendix B), since this area is crossed by political borders, and this makes the information contained in the Italian catalogue (PFGING) too incomplete for CN application. The period of time analysed for the Northern region (1964–1992) is chosen accordingly to the completeness level of the obtained catalogue, and the threshold for the selection of the events to be predicted is fixed to M_0=5.4. In the Central and Southern regions, the analysed period goes from 1954 to 1992, with M_0=5.6 and M_0=6.5, respectively. Further details concerning this analysis can be found in Costa et al. (1996). The results of predictions obtained for the two variants of the regionalization, including and excluding intersection domains (Fig. 6), are summarised in Table 3. The duration of TIPs is reduced when the areas of investigation partially overlap, thus it is reasonable to assume that the zones of intersection are involved in the preparation of the strong events and therefore must be included in the different areas of investigation.

The experiments performed for the Italian territory, briefly described so far, show that a choice of the areas of investigation supported by seismological and tectonic evidences permits to improve the stability of the algorithm, while reducing the percentage of TIPs and the failures to predict. This observation justifies tracing the boundaries of the areas strictly following the seismotectonic zoning, with the aim to reduce the time–space uncertainty of predictions (without increasing the failures to predict) and, at the same time, to decrease the subjectivity in the definition of the areas of investigation.

Accordingly, the regionalization (Fig. 7) currently used for the application of CN algorithm in Italy

Table 3
Results of CN retrospective application for the regionalization of Italy by Costa et al. (1996)

	North		Centre		South	
	Area 1	Area 2	Area 1	Area 2	Area 1	Area 2
Events predicted/total	2/2	2/2	3/3	3/4	3/3	1/2
False alarms	1	2	2	4	5	2
TIP (%)	27	34	23	38	33	25

Area 1—including intersection domains.
Area 2—excluding intersection domains.

(Peresan et al., 1999a), has been defined following closely the seismotectonic zones (Meletti et al., 2000), independently defined by GNDT (Gruppo Nazionale per la Difesa dai Terremoti), and taking into account the main geodynamic features of the Italian area. Considering the general rules for CN application (described in Section 2.1) and the sizes of the seismogenic zones, these zones have been grouped according to their seismogenic regime and to the available geodynamical information. Each area of investigation includes only zones with the same seismogenic characteristics (e.g. only compressive or only extensive) and the adjacent zones with transitional properties. A transitional zone has been included in the area of investigation only if it is between zones of the same kind, or if it is located at the edges of the area and the space distribution of the aftershocks reveals a possible connection. For this purpose, the identification of aftershocks has been performed with the "minimax" method, proposed by Molchan and Dmitrieva (1992).

Several different configurations of the areas of investigation have been tested, as comprehensively described in Peresan et al. (1999a), and the resulting regionalization covers a large part of the Italian territory, including the most seismically active areas. However, some zones, such as the Western Alps and the African/Adriatic foreland zones, in Southern Sicily and in the Gargano region, could not be included in the analysis, due to their low seismic activity, which did not allow for CN application thus far.

The rules for the definition of CN regionalization based on the seismotectonic zoning, permit to account for the available independent information provided by geology and geodynamics, and not only by seismological observations. This appears especially important in view of the complex geodynamic framework of the Italian peninsula, where extremely fragmented and heterogeneous seismogenic structures coexist within a short distance. The idea to consider groups of homogeneous seismogenic zones, with the aim to optimize the selection of the casual system of faults involved in the preparation process, as proposed by Peresan et al. (1999a), was successful, although at first sight controversial with respect to previous standard applications (e.g. Rotwain and Novikova, 1999). The necessity of grouping the

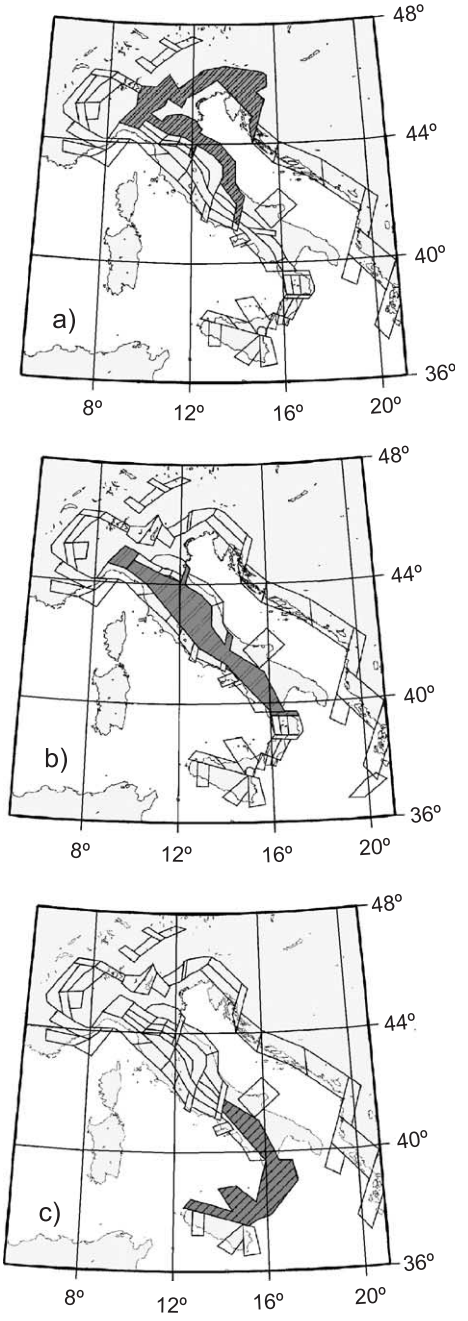

Fig. 7. Regionalization of the Italian territory proposed by the Peresan et al. (1999a) and following closely the seismotectonic model (Meletti et al., 2000). (a) Northern Region; (b) Central Region; (c) Southern Region.

seismogenic zones, moreover, seems supported by the unsatisfactory predictive capability provided by an attempt to forecast the occurrence of large crustal events within individual seismogenic zones (Boschi et al., 1995b).

3.2. Stability tests

The stability of the results with respect to the choice of the free parameters of the algorithm (Costa et al., 1995), as well as to the definition of the area of investigation (Costa et al., 1995; Peresan et al., 1999a), and against possible errors in the input data, such as systematic (Peresan et al., 2000) and random errors (Peresan et al., 2002) in the reported magnitudes, has been tested.

The regionalization supported by tectonic and kinematic arguments permits to increase the stability of results while reducing the space–time uncertainty of predictions.

The analysis of the effect of random errors in magnitude on CN predictions, shows that a stable prediction is assured if the threshold-setting period corresponds to a time interval sufficiently long and representative of the seismic activity within the area of investigation, including periods of quiescence as well as periods of high activity (Peresan et al., 2002). Consequently, for the forward monitoring the thresholds setting period for CN application to the Italian territory has been extended (since January 1999) up to December 1998.

The careful analysis of CN functions permitted to detect a relevant long-lasting undeclared change in the magnitudes reported in the ING bulletins (Peresan et al., 2000), starting approximately in 1987. Such inhomogeneity prevented their use for the routine monitoring of seismicity with CN and made it necessary to compile the UCI2001 catalogue (Peresan and Panza, 2002), which is updated using the NEIC global catalogue since 1986, as described in Appendix B. A series of experiments, performed systematically increasing or decreasing the operating magnitude, showed that it is possible to distinguish the effects of such variations from the anomalies in the seismic flow that define the TIPs for the occurrence of a strong event (Peresan et al., 2000). On the other hand, short-term inadvertent increase in reported magnitude, indicated by Zuniga and Wyss (1995) for the Italian catalogue, does not seem to affect the results of predictions (Peresan et al., 1999a).

3.3. Forward monitoring

Taking into account the results of the comprehensive testing of the stability of CN performances in Italy, the experimental real-time prediction of earthquakes initiated in January 1998. In fact, provided that the data are regularly updated (i.e. with a time delay shorter than a couple of weeks), it is possible to issue predictions that can be tested in real-time against the subsequent occurrence of strong events.

The analysis of seismicity is performed within the three investigation areas shown in Fig. 7 (Peresan et al., 1999a,b), very roughly corresponding to the Northern, Central and Southern parts of the Italian territory. The thresholds M_0 for the selection of the events to be predicted are fixed, taking into account their average return period, to M_0=5.4 for the Northern region and to M_0=5.6 for the Central and Southern regions. Predictions are routinely updated every 2 months using, since January 1999, the UCI2001 catalogue. The results updated to November 1, 2003, are shown in Fig. 8. A complete archive of predictions, obtained both in retrospective analysis (i.e. for the periods 1954–1997 in the Central and Southern regions, and 1964–1997 for the Northern region) and in forward predictions (since January 1998), can be viewed at http://www.ictp.trieste.it/www_users/sand/prediction/prediction.htm.

Since the beginning of the experimental real-time prediction of earthquakes, in January 1998, three strong earthquakes occurred within the areas monitored by CN algorithm (Fig. 7). The Bovec event (M=6.0), which occurred in April 12, 1998 in the Slovenian territory, was preceded by a TIP declared for the Northern region starting on November 1996. The Pollino earthquake (M=5.7), which occurred in September 9, 1998, and located in the overlapping part of the Central and Southern regions, was correctly predicted in the context of the Central region, while it was a failure to predict in Southern Italy (possibly due to the low completeness level of the catalogue in this region, as discussed in Appendix C). Finally, the recent Monghidoro earthquake (M=5.5), which occurred in September 14, 2003,

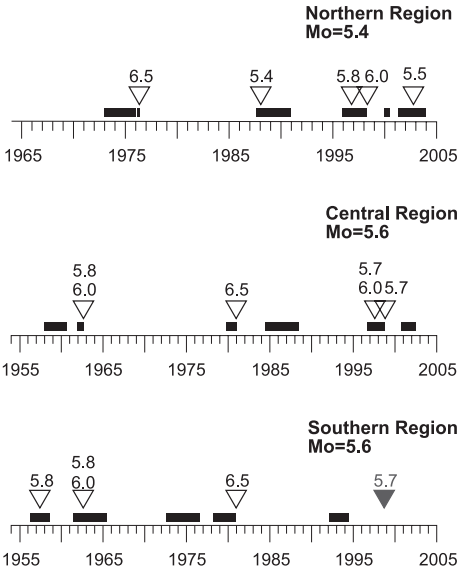

Fig. 8. Diagrams of the Time of Increased Probability (TIPs) obtained for the three Italian areas of investigation in the monitoring of seismicity (updated to November 1, 2003). Black boxes represent the periods of alarm, while a triangle with a number above indicates the occurrence of a strong event together with its magnitude. The catalogue used for the monitoring up to December 1998 was the CCI1996, integrated with NEIC and ALPOR data; since January 1999 predictions were updated using the UCI2001 catalogue (see Appendix B).

was a successful prediction in the Northern region, as the July 12, 2004, M=5.6 event in Slovenia. These results, still providing a limited sample, are rather encouraging and appear to substantiate the predictive capability of the algorithm CN in Italy, as inferred by the retrospective analysis of seismicity.

The space–time volume occupied by alarms is estimated following Kossobokov et al. (1999b), that is taking into account the space distribution of epicenters in the monitored territory. At each given time, the percentage of space occupied by alarms is estimated as the ratio of the number of epicenters from a sample catalogue (e.g. catalogue of events with M>4.0, which is expected to be complete and representative over the whole time interval), which fall inside the alerted area, versus the total number of epicenters included in the monitored territory (union of the three areas of investigation for CN application). In such a way, an area of given size characterised by low seismic activity (small number of events from the sample catalogue), will be

Table 4
Space and time uncertainties and score of CN predictions in Italy (updated to November 1, 2003)

Area	Time (%)	n/N	Space (%)
Northern region	29	5/5	37
Central region	24	6/6	53
Southern region	29	4/5	25

associated with a large space uncertainty, while areas of similar size, but characterised by higher concentration of epicenters (large number of events), will provide a lower space uncertainty. In fact, the certainty of a distribution is higher when a larger sample is used for its reconstruction. The space and time uncertainties associated to each of the three areas of investigation shown in Fig. 7, as well as the score of predictions, are reported in Table 4. The time uncertainty, i.e. the percentage of time occupied by alarms, is estimated as the ratio A/T, where A is the total duration of alarms and T is the total time of analysis. The percentage of space corresponding to each of the CN areas shown in Fig. 7 is estimated as s/S, where s is the total number of epicenters included in the area of investigation and S is the total number of epicenters included in the monitored territory. All events with $M\geq$4.0 from the UCI2001 catalogues, in the period 1950–2001, are considered. Because of the overlapping of the areas of investigation, the sum of the three numbers exceeds 100%. One should account for this proportion when making judgment of the performances of the algorithm in Italy. The space–time volume of alarm is finally computed as the average spatial percentage of alarm over the total period of diagnosis, considering both retrospective simulation and real-time predictions. The score of CN algorithm, both in retrospective analyses and advance predictions, is given as the ratio n/N, where n is the number of predicted events and N is the total number of strong events (Fig. 8). The ratio n/N, is computed counting only once the earthquakes which occurred at the intersections of the areas of investigation. The estimation of the space–time volume of alarms and the score of CN predictions in Italy (as on November 1, 2003), evaluated taking into account the space distribution of epicenters in the monitored areas (Fig. 7), are summarised in Table 5. During the period 1954–1963 (retrospective simula-

Table 5
Space–time volume of alarm in CN application in Italy (updated to November 1, 2003)

Experiment	Space–time volume of alarm (%)	n/N
Retrospective[a] (1954–1963)	41	3/3
Retrospective (1964–1997)	27	5/5
Forward (1998–2003)	46	3/3
All together (1954–2003)	31	11/11

[a] Central and Southern regions only.

tion) only the Central and Southern regions are considered. All of the events that occurred inside the regions of investigation are preceded by TIPs in at least one of the monitored areas.

4. Algorithm M8 in Italy

The first prediction of M8 algorithm to the Apennines (Keilis-Borok and Kossobokov, 1990) considered M_0=6.5 and the period 1970–1986. The only strong earthquake, Irpinia, November 23, 1980, was predicted in the retrospective simulation. The Italian catalogue of comparable completeness is not available for us in a real-time mode. Therefore, a real-time testing of M8 algorithm in Italy requires the use of another seismic database as well as a modification of the algorithm per se.

Later on, the algorithm M8 was applied retrospectively to the territory of Italy with M_0=6.0 and M_0=6.5 (Romashkova et al., 1998), using the PFGING catalogue (Peresan et al., 1997 and references therein). In the retrospective simulation, the algorithm was run each half-year from 1972 to July 1995. The circles of investigation, CI's, were distributed along the line of maximal concentration seismic epicenters with approximately three-times-overlap, so as to cover all the seismicity of the region (Fig. 9). The location of the CI's and their number (14 CI's with R=192 km for M_0=6.5, and 16 CI's with R=138 km for M_0=6.0) was different for M_0=6.5 and M_0=6.0, in order to provide approximately the same degree of their overlap in these two cases. The completeness of the PFGING catalogue allowed the application of the modified version of the M8 algorithm only. The modification reduces the value of the requested recurrence rate of main shocks in the areas of investigation, $\tilde{N}$, from the standard 20 events per year to a smaller number. All the remaining parameters of the algorithm are not changed, thus reducing the potential freedom of data fitting to one dimension. In the retrospective simulation, three out of the four strong earthquakes were predicted and the alarm occupied about 30–40% of the total space–time volume.

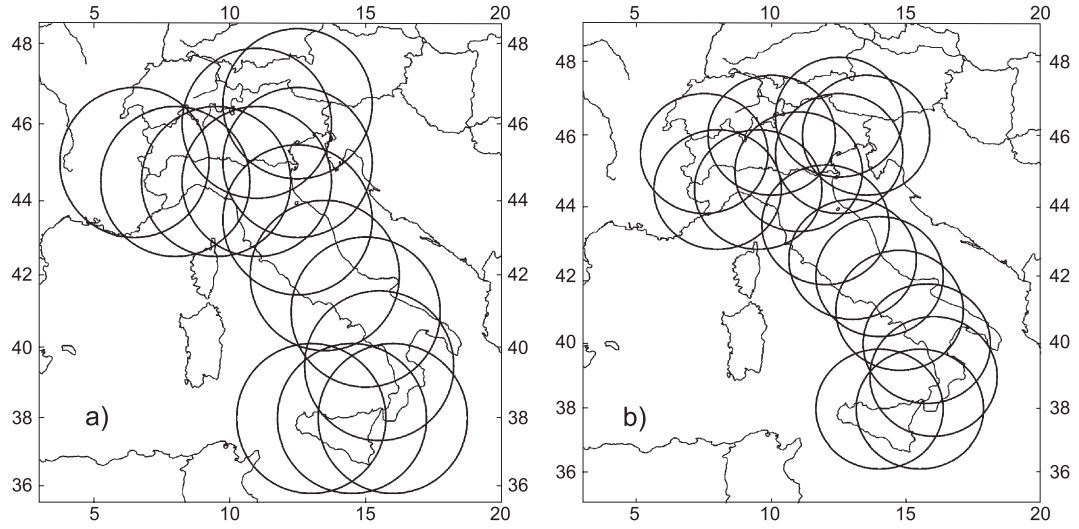

Fig. 9. Circles used by Romashkova et al. (1998), in the application of algorithm M8 for the prediction of earthquakes in the magnitude range M6.5+ (a) and M6.0+ (b) in Italy.

Table 6
Results of M8S retrospective application in Italy and adjacent territory, 1972–2001

Date	Latitude, °N	Longitude, °E	Depth	M	M8S	Commentary
May 06, 1976	46.23	13.13	12	6.5	yes	
November 23, 1980	40.85	15.28	18	6.7	yes	
September 26, 1997	43.08	12.81	10	6.4	no	Predicted in M5.5+
April 12, 1998	46.24	13.65	10	6.0	yes	Slovenia
January 16, 1975	38.20	15.78	21	5.5	yes	
April 15, 1978	38.27	15.10	18	5.8	yes	
September 19, 1979	42.72	12.95	6	5.8	no	20 km from alarm
May 28, 1980	38.46	14.34	19	5.5	yes	
November 25, 1986	44.12	16.34	30	5.5	no	Croatia
May 05, 1990	40.78	15.77	10	5.6	yes	
November 27, 1990	43.85	16.63	24	5.6	no	Croatia
February 26, 1991	40.19	13.82	401	5.5	no	deep event
January 05, 1994	39.08	15.15	272	5.8	no	deep event
October 15, 1996	44.79	10.78	10	5.8	yes	
September 26, 1997	43.05	12.88	10	5.9	yes	
May 18, 1998	39.25	15.11	279	5.6	yes	deep event
September 09, 1998	40.03	15.98	10	5.9	yes	
July 17, 2001	46.73	11.20	10	5.5	yes	

As with CN, the spatial percentage of alarm at each given time, is computed as the ratio of the number of epicenters from the sample catalogue, which fall inside the area of alarm, to the total number of epicenters, which fall inside the union of all circles of investigation. The space–time volume of alarm is then

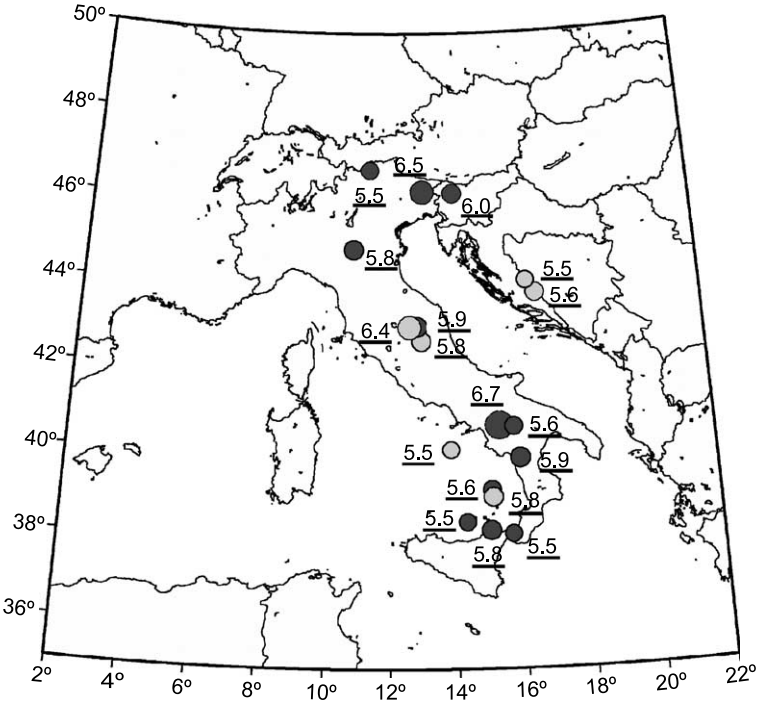

Fig. 10. The main shocks, with $M \geq 5.5$, in Italy and adjacent territory as reported in UCI2001, during the time interval 1972–2001 (Table 6). The black circles show the epicenters of the earthquakes predicted by M8S algorithm, the grey circles the missed ones. The size of the circles is proportional to their magnitude.

computed as the average spatial percentage of alarm over the total period of diagnosis (Kossobokov et al., 1999b).

In 2000, the next application of the M8 algorithm to the territory of Italy was performed for M_0=6.5 and M_0=6.0, using the catalogue CCI1996, updated by data from NEIC (Peresan et al., 1999b). All the parameters of the algorithm, including the position of the CI's remained the same as in the experiment of Romashkova et al. (1998). In the retrospective simulation, three out of the four large earthquakes were predicted. The space–time volume of alarm diminished by a few percent.

At present, a new revised catalogue, called UCI2001 is available (Peresan and Panza, 2002). The catalogue UCI2001 is precisely the same as the one used by algorithm CN (see Section 3); the only difference is in the way the operating magnitude is defined in two algorithms. The M8S algorithm works with the maximum reported magnitude ($M_{\max}$), whereas the CN algorithm uses the determination based on priority (as described in Appendix B). For the sake of simplicity, in this section we will refer to $M_{\max}$ simply as M.

The M8S algorithm, has been applied (Kossobokov et al., 2002 and references therein) to the Italian data, within 38°N–47°N and 7°E–17°E, to simulate retroactively a forward prediction experiment from January 1972 to January 2002, using the catalogue UCI2001. The predictions are performed in three consequent magnitude ranges defined by M_0=6.5, 6.0 and 5.5, referred to as M6.5+. M6.0+ and M5.5+ from now on. The following values of the parameters, described in Section 2.2.2, are fixed in the application of M8S in Italy: r=28 km, a=0.3 main shocks of magnitude 3 or higher per year, s equals the linear dimension of the target earthquakes, n=75% of the remaining neighboring grid points from a 3×3-grid square. Of course, the choice of these parameters could be different in different regions and we recommend varying them when designing a new test,

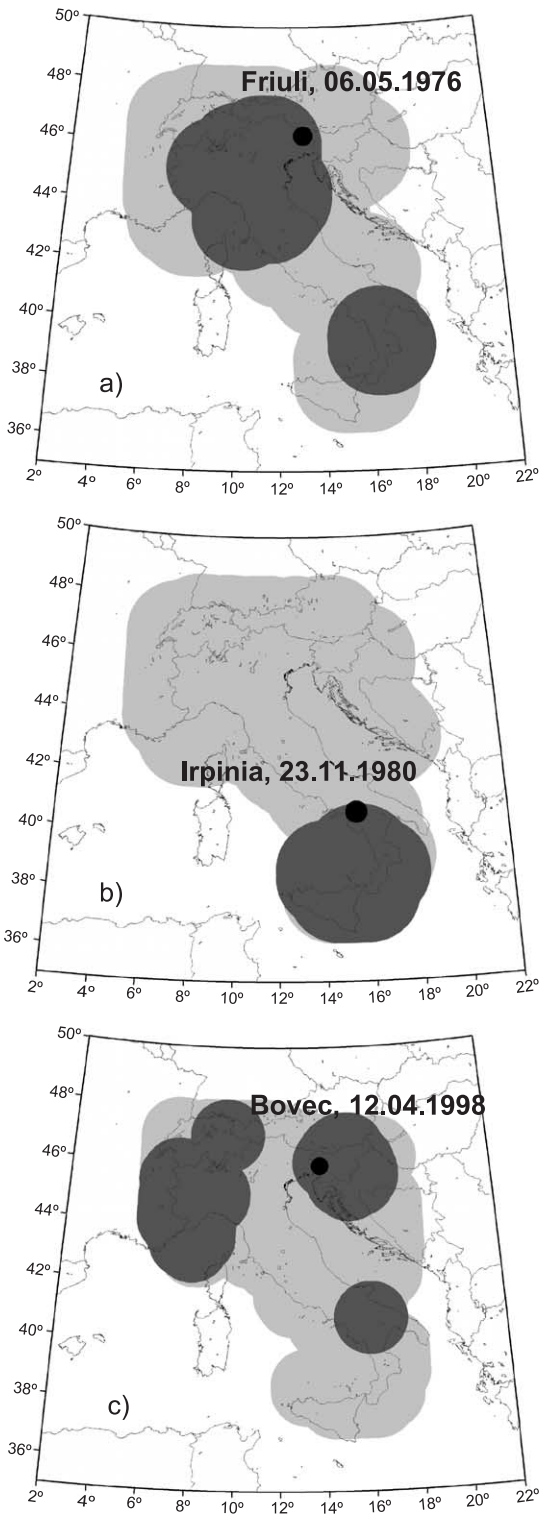

Fig. 11. Results of predictions obtained with the M8S algorithm for M6.5+ for (a) the Friuli 1976, M=6.5, and (b) the Irpinia 1980, M=6.7 earthquakes. (c) Same for M6.0+ for the Bovec 1998, M=6.0 earthquake. The light grey circles outline the territory monitored with the algorithm M8S; the dark grey circles display the alarm area.

in order to obtain the most stable results of the retrospective simulation.

The possibility of considering different magnitude ranges (i.e. regions with different levels of seismicity) is provided in the algorithm M8 by means of the normalization of its internal parameters. This normalization is based on the general concept that determines the interrelation between the space–time scale of the earthquake preparation process and the size of the incipient large event. Thus, within the framework of the self-similarity hypothesis for the seismic activity, there isn't any formal difficulty to the application of M8 for the prediction of both the strongest events and the earthquakes of moderate size. On the other hand the earthquake are by no means absolutely independent events. In general, the seismic activity, so-called *seismic flow*, can be considered as a multiscale association of the hierarchical self-organised individual earthquake preparation processes (Molchan et al., 1997), which are strongly interfering. Therefore, the effectiveness of moderate magnitude events prediction strongly depends on the current situation, with regard to earthquake preparation processes at higher levels of hierarchy.

Table 6 gives the list of the target earthquakes as reported in catalogue UCI2001 in 1972–2001 and the result of M8S retrospective simulation. There are 18 main shocks with $M \geq 5.5$ inside the considered area (Fig. 10). Fifteen of them occurred in Italy, one earthquake near its border (Bovec, Slovenia) and two earthquakes on the territory of Croatia.

Fig. 11 illustrates the results of M6.5+ and M6.0+ tests in Italy. Both the strongest Italian earthquakes—Friuli May 06, 1976, M=6.5 and Irpinia November 23, 1980, M=6.7—are predicted in the M6.5+ test. In the M6.0+ test, one earthquake—Bovec April 12, 1998, M=6.0—is predicted and the other earthquake—Assisi September 26, 1997, M=6.4—is missed.

In the M5.5+ test, 9 out of 14 earthquakes are predicted. Among the missed earthquakes are the two Croatian events—November 25, 1986, M=5.5 and November 27, 1990, M=5.6—and the two deep ones—February 26, 1991, M=5.5 and January 05, 1994, M=5.8. The earthquake 1979.09.19, M=5.8, happened about 20 km from the alarm area.

Table 7
Space–time volume of alarm in M8S applications in Italy (1972–2001)

Experiment	Space–time volume of alarm (%)	
	All shocks	Area
M6.5+	36	28
M6.0+	40	37
M5.5+	39	38

The space–time volume of alarm in M8S applications, aimed at the prediction of earthquakes from the three subsequent magnitude ranges, M6.5+, M6.0+ and M5.5+, are shown in Table 7. In these tests, the average space–time volume of the alarm, as a percentage of the total is about 36–40% when the space area weighted on seismic activity is used for the computation of this volume, and it is about 28–38% when the space area in km^2 is considered.

Fig. 12 illustrates the time evolution of the space volume of alarm in the prediction experiments for M6.5+, M6.0+ and M5.5+. The variations of the alarm percentage, estimated either with the area weighted on seismic activity or with the area computed in km^2, are close to each other. The graphs for M6.5+, M6.0+ and M5.5+ show a similar evolution; nevertheless, only the M6.5+ test presents an absolutely quiet period, from July 1985 to January 1989. In all tests, a rather large territory in state of alarm may be observed at the beginning of the investigated period. This alarm is associated with the Friuli May 06, 1976, M=6.5 earthquake. Then the percentage of alarm area diminishes gradually and reaches minimum values in 1985–1990. In 1990–1995 one can see an escalation in the alarm area. All these alarms turned out to be false. After 1996 the rather high level of alarm is partly confirmed by the occurrence of six strong earthquakes—the Bovec April 12, 1998, M=6.0 earthquake in the M6.0+ test, and five earthquakes in the M5.5+ test. The Assisi earthquake, which was a failure to predict for M6.0+, falls inside the alarm area of the M5.5+ test. The

Fig. 12. Time evolution of the space–time volume of alarm for: (a) M6.5+; (b) M6.0+; (c) M5.5+. The two curves correspond to the different methods used for the space–time volume estimation (see Section 4): the lines with rectangles correspond to the area computed in km^2; the lines with triangles correspond to the space weighted on seismic activity. The subcatalogue of all earthquakes with $M \geq 4.0$ from the UCI2001 catalogue, in the period 1950–2001, is used as representative of the seismic activity.

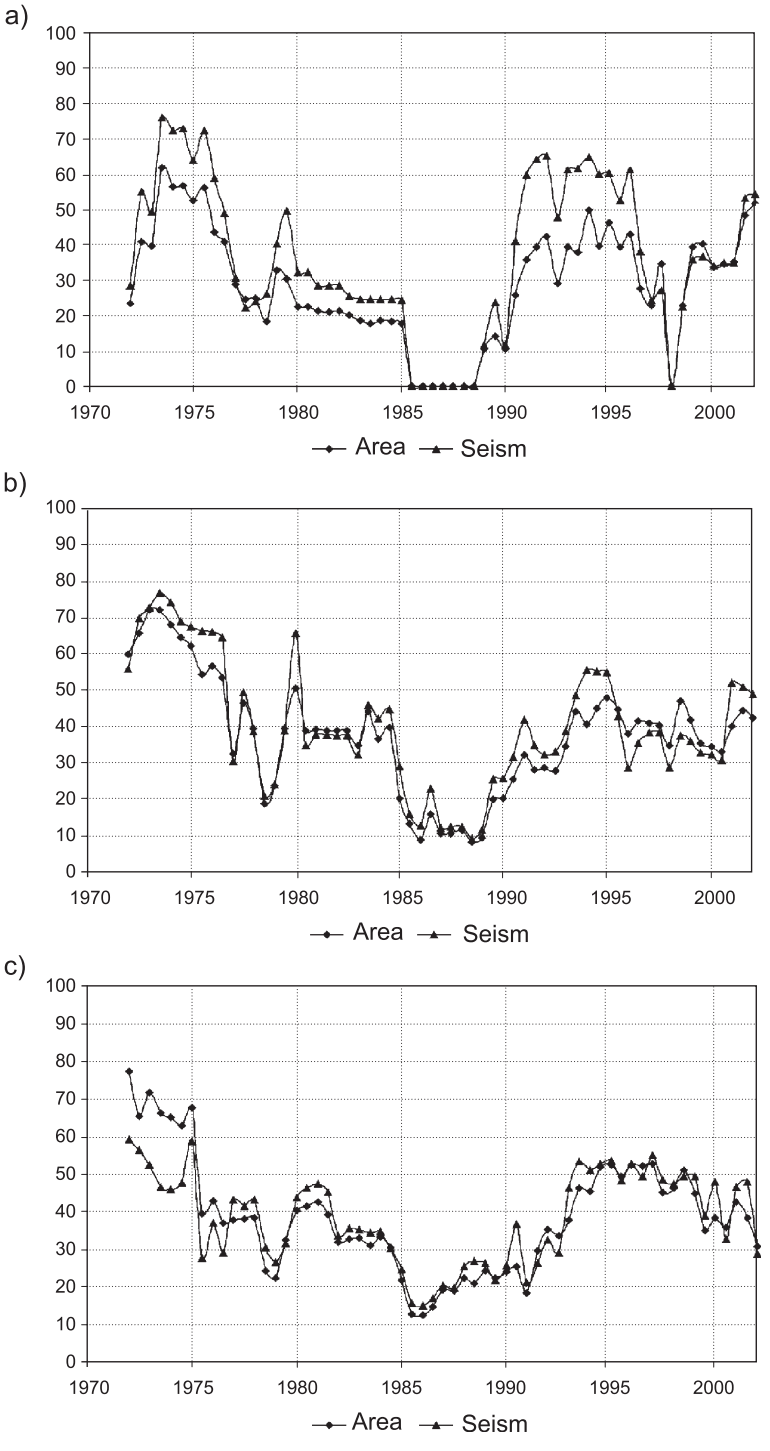
a)
100
90
80
70
60
50
40
30
20
10
0
1970
1975
1980
1985
1990
1995
2000
Area
Seism
b)
100
90
80
70
60
50
40
30
20
10
0
1970
1975
1980
1985
1990
1995
2000
Area
Seism
c)
100
90
80
70
60
50
40
30
20
10
0
1970
1975
1980
1985
1990
1995
2000
Area
Seism

cases of the missed earthquakes are discussed in Appendix C.

The presented retrospective result of M8S algorithm application seems to be rather encouraging: 12 out of 18earthquakes with magnitude 5.5 and more are predicted within about one-third of space–time volume. These tests become the starting point of the experimental real-time prediction of earthquakes from subsequent magnitude ranges in Italy, which was set up in January 2002. In fact, as for the algorithm CN, if the data are available with a sufficiently short time delay (about a couple of weeks), it is possible to issue predictions, which could be tested in real-time against the subsequent occurrences of strong events.

Since January 2002 and to the end of 2003, no main shocks of magnitude 6.0 and more happened inside the investigated territory. At the same time, four main shocks of magnitude between 5.5 and 6.0 happened there: an earthquake of M=5.9 offshore Sicily (September 06, 2002), another one with M=5.9 in Molise region (October 31, 2002), the third one with M=5.5 offshore of Croatia (March 29, 2003), and the fourth one with M=5.6 about 20 km from Bologna (September 14, 2003). The first two main shocks are missed by M8S, while the second two are predicted.

Fig. 13 shows the alerted areas as stated from prediction on July 01, 2003. There is a rather extensive territory in state of alarm in the northern part of Italy both for M6.5+ and for M6.0+. The area for M6.5+ is larger. It spreads from the Marche–Umbria region to the North, covering the Alps and adjacent territory. The area for M6.0+ is a little narrower and excludes the regions of Friuli and Dolomites, and Italy–Switzerland border neighborhood. The situation with the M5.5+ alarm is more complicated. The main alarm area is situated on the north of the Italian peninsula. This alarm has been confirmed by the recent Loiano–Monghidoro–Monzuno (near Bologna) earthquake happened on September 14, 2003.

After the paper's submission another targeted earthquake took place within the territory alarmed

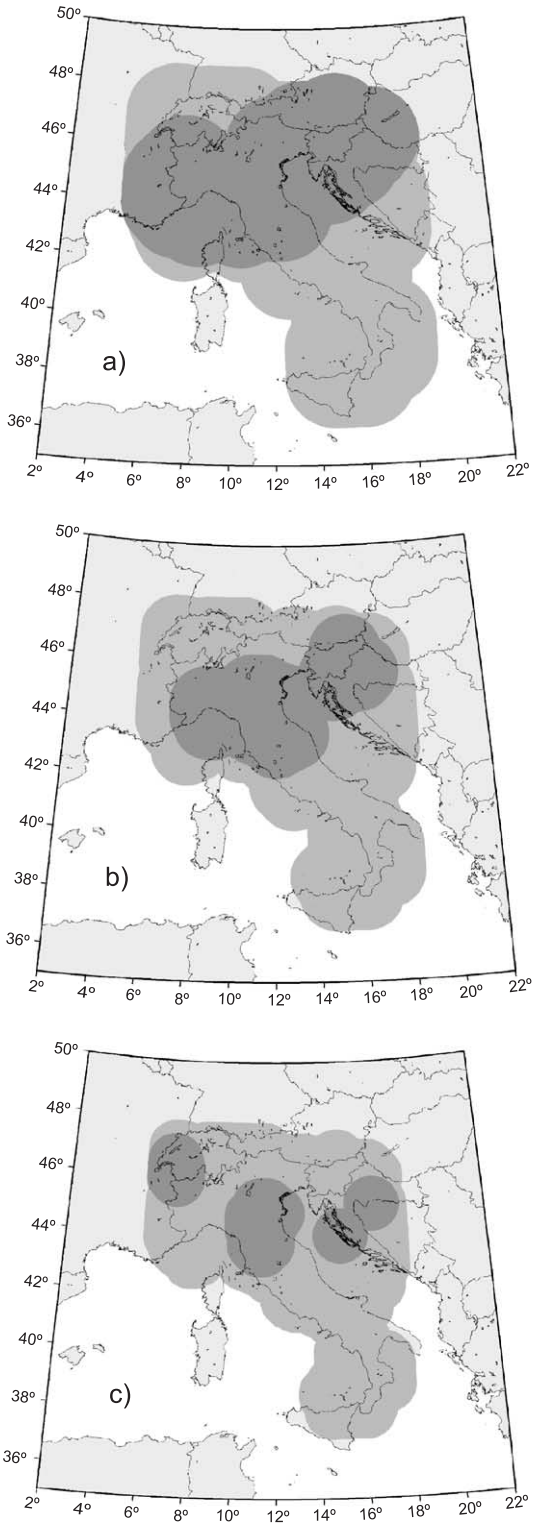

Fig. 13. M8S predictions as on January 7, 2003 for the three magnitude ranges (a) M6.5+; (b) M6.0+; (c) M5.5+. The light grey circles outline the monitored territory; the dark grey circles display the alarm area.

by M8S algorithm; the M=5.5 event, occurred on February 23, 2004 near the France–Switzerland border, has been successfully predicted. Thus, all of the three alerted areas for M5.5+, shown in Fig. 13c, have been subsequently validated by the occurrence of strong earthquakes. However, the most recent July 12, 2004, Slovenia earthquake, with preliminary M_{max}=5.6, took place outside the M8S alarmed areas, similar to the two earthquakes, which previously occurred in the southern part of Italy were missed (possibly due to the insufficient level of completeness of the catalogue in this region, as discussed in Appendix C). The full archive of results since 1985, both in retrospective simulation and real-time prediction, can be viewed at http://www.ictp.trieste.it/www_user/sand/prediction/prediction.htm.

5. Discussion and conclusion

The reproducible earthquake prediction algorithm CN and M8 fully agree with the general definition suggested by Allen et al. (1976) and essentially provide predictions of intermediate-term middle-range accuracy. One of the crucial points in earthquake prediction is the statistical evaluation of the effectiveness of predictions, taking into account the posterior adjustments of the hypothesis in retrospective tests. Only a full specified prospective test can really overcome this problem, though, given the long return period of strong earthquakes at a certain location, not less than 30 years are necessary to collect statistically significant evidences for a given prediction strategy (Gusev, 1998). A possible alternative is to consider altogether the results of predictions from different locations, hence assuming that precursor of large earthquakes are the same worldwide, despite the large variability of the faulting environment from region to region (e.g. Kossobokov et al., 1999b; Rotwain and Novikova, 1999). The algorithms M8 and CN, in fact, fulfil the necessary preconditions for a scientific testing: (1) their ultimate description, that is the computer code, was published and distributed since its origination (Healy et al., 1992; Kossobokov, 1997); (2) at least some of the routine seismic catalogues are complete enough for a real-time application of "black box" version of the algorithms that guarantee the absence of human intervention; (3) the prediction results are unambiguous and permit an easy comparison with the null-hypothesis of random recurrence of earthquake epicenters in places where they were reported.

The intermediate-term middle-range predictions described in this paper are not associated to a specific value of probability for the occurrence of a strong earthquake. The simple definition of alarm periods as "times of increased probability with respect to normal conditions", is imposed by the fact that any attempt to quantify precisely the probability increase during TIPs would acquire several a priori assumptions (i.e. Poissonian recurrence, independence of TIPs and functions, etc.). Most of these assumptions would be poorly constrained by the available observations and hence below any critics.

The space–time uncertainty of intermediate-term middle-range predictions is intrinsically rather large and about 30% of the monitored space and time volume results in a state of alarm. Nevertheless, the uncertainty of predictions can be significantly reduced combining the outcomes from both CN and M8S algorithms.

The experiment of combining the predictions in Italy was done by Romashkova et al. (1998), although the comparison between the results obtained with M8 and CN (Costa et al., 1996) algorithms should be viewed as rather qualitative. This is due to the following differences of the two methods: (1) M8 uses a circle as the area for prediction while CN uses predefined areas of investigation: (2) many of the circles used by M8 overlap significantly while the three areas by CN either do not intersect at all or have a very limited intersection; (3) M8 and CN are applied to different, although overlapping, intervals of time; (4) magnitude thresholds selecting the events to be predicted and the operating magnitude scales (M_{max} for M8S and $M_{priority}$ for CN) are different. Despite of the differences, Romashkova et al. (1998) compared the results: (1) by limiting the predictions to the intersection between the circles used by M8 and the areas used by CN and to the time intervals in common; (2) by using the assigned table of correspondence between the values of M_0; (3) by distinguishing for a single space–time domain the four outcomes of prediction—both algorithms diagnose a TIP, both algorithms diagnose NO TIP, M8 diagnoses a TIP while CN does not, and, vice versa.

As a result, both earthquakes with magnitude 6.0 or larger fall into the space–time volume where both algorithms diagnose a TIP, which is predicted by both algorithms. Accordingly, it was suggested to declare an alarm of the M8 and CN combination in a space–time domain, if both algorithms diagnose a TIP in it. For the whole territory of Italy, this rule reduced the total space–time volume of TIP (measured accounting to background seismicity) from 22% for M8 and 24% for CN to 5% for their combination. The achieved numbers are natural empirical estimates of the probability of alarm for each of the two algorithms and their combination. It is notable that the product of the two probabilities defined for M8 and CN individually is very close to the probability for the M8 and CN combination, such as in the mathematical definition of independent variates. Therefore, apparently M8 and CN, despite their commonly accepted similarity, perform as independent experts. An example is provided by the strong earthquake M_{max}=5.6 that occurred in September 14, 2003, near Bologna, which was located inside the Northern region alerted by CN (Fig. 7a) and the areas alerted by M8S algorithm for the occurrence of events with magnitude larger than 5.5 (Fig. 13c); in this case, the space uncertainty (i.e. the territorial intersection of the areas alerted by the two algorithms, shown in Fig. 14) is significantly reduced to about 15% of territory monitored by both the algorithms.

Short-term predictions might appear the most useful at first glance; nevertheless, considering the problems related with the short-term prevention measures, such predictions should be provided with an extremely high precision, which is probably impossible to attain. On the contrary, the intermediate-term middle-range predictions, where alarms are declared for a time interval of a few years and with a space uncertainty of a few hundred kilometers, appear nowadays to represent a realistic goal (Kossobokov et al., 1999b; Keilis-Borok and Soloviev, 2003). Therefore, although the TIPs declared by the intermediate-term predictions by no means imply a "red alert", which could justify extreme actions (such

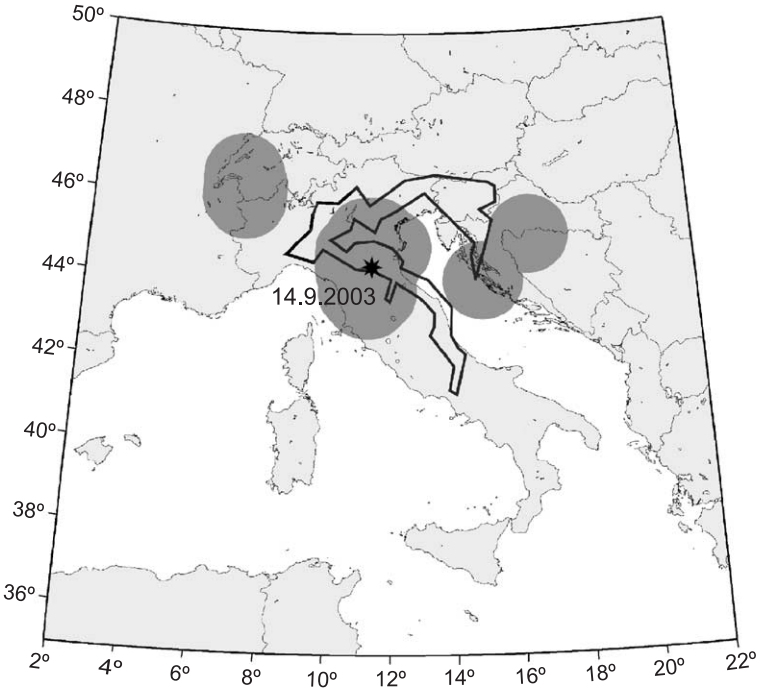

Fig. 14. Areas alerted by CN (delimited by the bold line) and by M8S (dark grey areas) for the occurrence of an earthquake with magnitude larger than 5.4 and 5.5, respectively, as on September 14, 2003, when a strong event (M_{max}=5.6) occurred. The epicenter of the earthquake is indicated by a star.

as the evacuation of people), the information provided by formally defined prediction algorithms may be useful to increase earthquake preparedness and to indicate possible priorities, to be followed in planning detailed seismic risk studies, which should be performed on a local scale (e.g. Correig, 2003). The practical utility of these predictions is to enable the relevant authorities to prepare for an impending destructive earthquake. A possible response could be, for example, an adequate planning of the emergency activities (e.g. placement and survey of the first-aid resources), thus allowing for well-coordinated, fast and efficient post-disaster rescue actions.

Acknowledgements

This work has greatly benefited from stimulating discussions with V.I. Keilis-Borok, I.M. Rotwain, I. Kuznetsov, G. Molchan, A. Soloviev and A. Correig. We are grateful to M. Caputo and to an anonymous reviewer for their very useful remarks. The research has been partly supported by the International Science and Technology Center (Project 1538-00), by the Russian Foundation for Basic Research (grant #00-15-98507), and by the James S. McDonnel Foundation (the 21st Century Collaborative Activity Award for Studying Complex Systems, project "Understanding and Prediction of Critical Transitions in Complex Systems"). This is a contribution to the MIUR-COFINANZIAMENTO projects 2001 and 2002, to the UNESCO-IUGS-IGCP Project 414 and to the NATO SFP project 972266. This study has been partly supported by the Regione Friuli-Venezia Giulia (funds for scientific research—year 2002).

Appendix A. Functions of the seismic flow

The non-independent *functions of the earthquake flow* illustrated in this section, allow us to describe and quantify the features of the contemporary seismic dynamics within a given area of investigation. These empirical functions evaluate the variations in seismic quiescence, space–time clustering of the seismic activity and spatial concentration of the earthquakes. Some of them may be related to well-known traits of seismicity, such as the Gutenberg–Richter relation, $\log N(M)=a-bM$ (where $N(M)$ is the cumulative number of events with magnitude larger than M and a,b are constants), or the Ormori law, $n(t)=K/(c+t)^p$ (where $n(t)$ denotes the occurrence rate of aftershocks at time t and K, c, p are constants), and permit to coarsely evaluate their variations. Most of the functions described in this section assume large values before the occurrence of a strong earthquake.

Robust trailing averages of the functions of the seismic flow, the so-called *traits*, are considered to define the *precursory seismicity pattern*. Different traits of seismicity can be represented by one or more different functions, or by the same function with different parameters (different time-window or different range of magnitude). The functions are estimated considering the sequence of main shocks; the number of aftershocks, however, is retained as one of the traits characterising the seismic sequence, by means of the function B.

The functions of the seismic flow estimated by CN are the following: $N1$, $N3$, K, G, Σ, $S_{\max}$, $Z_{\max}$, q, B, while those evaluated by the algorithm M8 and M8S include: N, L, Z (estimated for two different minimum magnitude cutoff) and B. Two of the CN functions, namely $N1$ and $N3$, are similar to the function N used by algorithm M8, although with a different choice of all the numerical values of the parameters. Actually, the functions $N1$ and $N3$ correspond to the same function, N, but are evaluated within different time intervals: $(t-s;\ t)$ and $(t-3s-1;\ t-2s-1)$, respectively. Also the function B is the same, both for CN, M8 and M8S, but it is estimated over different magnitude ranges. The functions $Z_{\max}$ and Z describe similar properties of seismicity, i.e. the ratio between the average linear dimension of the sources and the average distance among them; nevertheless, while CN takes into only the maximum value $Z_{\max}$, all of the values of Z are considered by M8 and M8S.

A.1. Level of seismic activity

Three functions (N, G and Σ) are used to describe the *level of seismic activity*. The function $N(t|\underline{M},\ s)$ corresponds to the number of earthquakes, with $M\geq\underline{M}$ and in time window $(t-s,\ t)$; G is the ratio of the

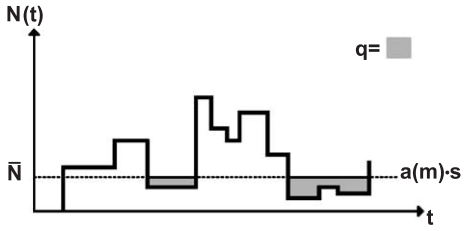

Fig. 15. Variation of the number of events as a function of the time, t The dotted horizontal line indicates the average number of events expected in the time interval of length s. The grey areas correspond to the periods of quiescence.

number of earthquakes in two different magnitude ranges: $m_1 \le M \le m_2$ and $M \ge m_1$

$$G(t|m_1, m_2, s) = 1 - \frac{N(t|m_2, s)}{N(t|m_1, s)} \qquad m_1 < m_2 \tag{5}$$

Σ evaluates the number of earthquakes, weighted according to their magnitudes, which occurred in the time interval $(t-s,\ t)$ and in the magnitude range $\underline{M} \le M_i \le \overline{M}$.

$$\sum(t|\underline{M}, \overline{M}, s, \alpha, \beta) = \sum_i 10^{\beta(M_i - \alpha)} \tag{6}$$

The function Σ may represent different physical quantities, depending on the value of β. Let us write the energy–magnitude relation in the form $\log E = A + BM$. In such a case:

- if $\beta \approx B/3$, then Σ is proportional to the total linear dimension of the earthquake sources;
- if $\beta \approx 2B/3$, then Σ is proportional to the total area of the sources;
- if $\beta \approx B$, then Σ is proportional to the seismic energy released.

The routinely used value in the algorithm CN is $\beta = B$.

A.2. Quiescence

One function, q, is used to describe the *quiescence*:

$$q(t|\underline{M}, s) = \sum_{+} \left[a\left(\underline{M}\right) s - N\left(t_i|\underline{M}, s\right) \right] \tag{7}$$

where $a(\underline{M})$ is the average yearly number of events. The sign $\sum_+$ indicates that the sum includes only the positive terms; therefore only the time intervals $(t_i - s,\ t_i)$, where the number of earthquakes is less than the average, are considered (Fig. 15).

In practice, $q(t|\underline{M}, s)$ corresponds to the sum of the grey areas shown in Fig. 15. The larger the value assumed by the function $q(t|\underline{M}, s)$ is, the more marked and prolonged the quiescence is.

A.3. Variations of seismic activity

Two functions, namely L and K, describe the *variations of seismic activity*. L represents the deviation of the seismic activity from the long-term trend, estimated for the time interval $(t_0,\ t)$:

$$L\left(t|\underline{M}, s\right) = N(t|\underline{M}, t - t_0) - N(t - s|\underline{M}, t - s - t_0)\frac{t - t_0}{t - s - t_0} \tag{8}$$

$N(t|\underline{M},\ t - t_0)$ is the number of events in the time interval $(t_0,\ t)$ and increases with t (Fig. 16); the second term in Eq. (8), instead, represents a linear extrapolation of the function $N(t)$ in the time interval $(t-s,\ t)$.

In the application of M8, t_0 generally corresponds to the beginning of the considered catalogue. Until recently, in fact, there was no possibility to define a long-term time window, due to the rather limited temporal span of the available catalogues; as time goes on, however, the size of catalogues will increase so that the function L will essentially duplicate N normalized to the constant long-term average. Hence,

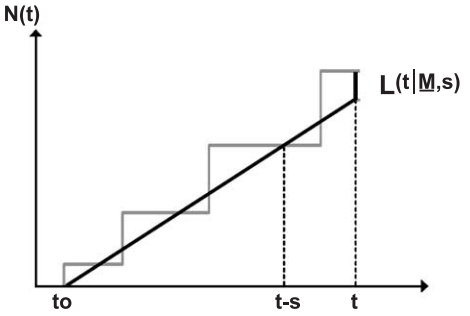

Fig. 16. Deviation of the seismic activity from the long-term trend: the segmented curve represents the real seismicity, while the line indicates the long period trend. The bold segment evidences the difference among the two quantities at time t.

in the algorithm M8S, a trailing time window, with fixed length of 30 years, has been introduced.

The function K corresponds to the *increment of seismic activity*, that is the difference between the number of earthquakes in two adjacent intervals of time, $(t-s,t)$ and $(t-2s, t-s)$, respectively.

$$K\left(t|\underline{M},s\right) = N\left(t|\underline{M},s\right) - N\left(t-s|\underline{M},s\right) \qquad (9)$$

Graphically, the function $K(t|\underline{M}, s)$ is represented by the difference between the areas, delimited by the curve $N(t)$, in two consecutive time windows (Fig. 17).

A.4. Clustering of earthquakes in space and time

The space and time clustering of earthquakes inside the area of investigation is represented by a single function. For each main shock, the number $b(e, M)$ of aftershocks with magnitude $M \geq \underline{M}$ is counted in the first e days after the main shock. The measure of clustering, B, is given by the maximum $b(e, M)$ for set $\{i\}$ of main shocks with magnitude $\underline{M}<M<\overline{M}$, occurring in the interval $(t-s', t)$:

$$B(t|\underline{M},\overline{M},s',M_{aft},e) = \max_{\{i\}}\{b_i(e,M)\} \qquad (10)$$

This function is used by CN, M8 and M8S algorithms, although with a different choice of parameters. The magnitude range considered by M8 and M8S, for example, is $(\underline{M}, \overline{M})=(M_0-p, M_0-q)$, where p and q are fixed parameters, while CN takes into account all the events with magnitude above the completeness threshold of the catalogue.

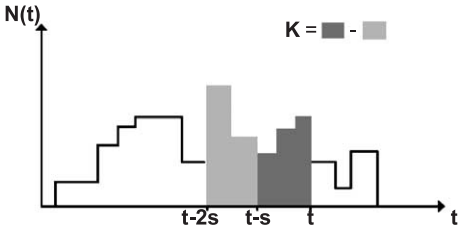

Fig. 17. Variation of the number of events as a function of time t; the two areas evidenced in grey correspond to the number of events in two subsequent intervals of length s. The function K is given by the difference among the two areas.

A.5. Space concentration of events

The space clustering of the earthquakes is described by the functions $S_{\max}$, $Z_{\max}$, for CN algorithm, and Z for M8 and M8S algorithms.

The function $S_{\max}$ is proportional to the average area of the source:

$$S_{\max}(t) = \max_j \left[\frac{\Sigma(t_j|\underline{M},\overline{M},s,\alpha,\beta)}{N\left(t_j|\underline{M},s\right) - N\left(t_j|\overline{M},s\right)}\right] \qquad (11)$$

with $\beta \approx 2B/3$, j=1,2,3.

As in the case of the function Σ (Eq. (6)), each term inside the parenthesis is related to the average fault area of the events with origin time t_i in the interval: $(t-j$ years$)\leq t_i \leq (t-(j-1)$ years$)$, B is from $\log E=A+BM$. $S_{\max}$ corresponds to the maximum value observed for such area during the 3 years that precede t.

The function $Z(t)=Z(t|\underline{M}, \overline{M}, s, \alpha, \beta)$ represents the linear concentration of the main shocks in the magnitude range $(\underline{M}; \overline{M})$ and time interval $(t-s; t)$, estimated as the ratio between the average linear dimension of the sources, l, and the average distance, r, between them. Usually, the average diameter of the source, l, is determined as $\frac{1}{N}\sum_{\{i\}} 10^{\beta(M_i-\alpha)}$, where N is the number of main shocks in $\{i\}$, $\beta \approx B/3=0.46$, and $\alpha=0$ (which does not restrict generality), while the average distance, r, between them is set proportional to $3\sqrt{1/N}$. It has been shown that the use of a more accurate estimate of the linear concentration of main shocks may improve the performance of the M8 algorithm (Romashkova and Kossobokov, 1996).

The maximum value, $Z_{\max}$, observed for the function Z in the 3 years preceding t, is considered by CN:

$$Z_{\max}(t) = \max_j \left[\frac{\Sigma(t_j|\underline{M},\overline{M},s,\alpha,\beta)}{\left(N\left(t_j|\underline{M},s\right) - N\left(t_j|\overline{M},s\right)\right)^{\frac{2}{3}}}\right] \qquad (12)$$

with $\beta \approx B/3$, j=1,2,3…

This function of CN algorithm is practically identical to $S_{\max}(t)$, except for the value of β.

A.6. Normalization of the functions

The functions of the earthquake flow are normalized, so that the integral traits of the seismic activity can be quantified uniformly, with the same set of parameters, even in areas with different sizes and levels of seismicity. The possibility of such normalization is practically relevant in connection with the problem of self-similarity of the earthquake flow and, consequently, of the seismic precursors. The normalization permits a uniform analysis of seismicity in different regions, thus allowing for an extensive test of the premonitory seismicity patterns and for a quantitative comparison of the seismic sequence in seismically different areas (Keilis-Borok and Rotwain, 1990).

The normalization is achieved by the choice of the magnitude range, $\underline{M} \leq M \leq \overline{M}$, for the events to be used in the computation of the functions; essentially, the minimum magnitude cut-off $\underline{M}$ is fixed in order to provide a sort of equalization of the seismic flow. Thanks to the normalization of the functions, the same set of standard parameters, fixed a priori by detailed analysis of seismicity in a given region, can be used in areas with a different level of seismic activity, without any ad hoc adjustment.

Appendix B. The earthquake catalogue

The intermediate-term middle-range prediction algorithms described in Section 2, require an input catalogue as complete and homogeneous as possible over the monitored territory. Besides, the catalogue must be updated rapidly enough to permit to issue predictions. If the data are available with a time delay not larger than a couple of weeks, we can define our results as real-time predictions.

The Italian catalogue of earthquakes is the result of several subsequent revisions and different stages characterised its compilation. The data set initially used for intermediate-term middle-range prediction purposes was obtained by Keilis-Borok et al. (1990) integrating the catalogues ENEL and ING (see Caputo, 2000 and references therein) with the events reported by the CSEM (European-Mediterranean Data File 1976–1988, Strasbourg, 1989). The analysis of the catalogue, preliminary to the application of the algorithm CN, evidenced that before 1971 many events had no assigned magnitude; since their number was almost equal to that of events with $M \geq 3.0$ which occurred after 1971, it was established to assign $M=3.0$ to all the events reported without any magnitude up to 1971. Such "homogenisation" of magnitudes was justified observing that the detection level should not allow to record smaller events in that time (Keilis-Borok et al., 1990).

In a second step, the ENEL+CSEM data were replaced by the PFG catalogue (Progetto Finalizzato Geodinamica; Postpischl, 1985), resulting from the integration and revision of the data available for the Italian territory. Thus, the PFGING catalogue (Costa et al., 1995) was assembled updating the PFG catalogue (time interval: 1000–1979) with the ING bulletins (available for the time interval 1980–July 1997).

Later on, the Current Catalogue of Italy CCI1996 (Peresan et al., 1997) was issued, which consists of a revised version of the PFGING catalogue, incorporating the information provided by the ISC bulletins (International Seismological Centre; 1976–1990) and by the CFT catalogue ("Catalogue dei Forti Terremoti in Italia dal 461 a.C. al 1980"; Boschi et al., 1995a). The revision has been performed at first on the basis of the information from ISC bulletins (1976–1990) in order to correct depth, magnitude and obvious errors in coordinates determinations. After that the origin time, coordinates and intensities were corrected according to the CFT estimations in the time period 1000–1980.

A unified and updated catalogue, the Updated Catalogue of Italy, UCI2001 (Peresan and Panza, 2002), is currently used for the routine monitoring of seismicity, for earthquake prediction purposes, in the Italian area. The compilation of the UCI2001, which consists of an updated and revised version of the CCI1996 catalogue, was necessary for the following two reasons:

1. A comparison of the bulletins compiled at the Istituto Nazionale di Geofisica (ING) with other seismic data sources (Peresan et al., 2000) evidenced the necessity to update the CCI1996 with a different data set, at least since 1986, due to relevant inhomogeneities in the reported magnitudes. In fact, the ING bulletins, turned out to be biased by a relevant underestimation of

the local magnitudes, starting approximately in 1987 and this prevents their use for the routine monitoring of seismicity.

2. All of the considered Italian catalogues (CCI1996, CFT and ING bulletins) cover an area that, toward the North, is fairly incomplete for the seismicity monitoring of the Italian territory, mainly due to the presence of many different political borders across the Alpine arc.

These problems have been solved by properly merging (Costa et al., 1996), up to 1985, the CCI1996, the NEIC (GHDB, 1989) and ALPOR (Catalogo delle Alpi Orientali, 1987) catalogues into the UCI2001 catalogue (Peresan and Panza, 2002) as follows:

- the subcatalogue of events contained in the PFG polygon (Postpischl, 1985) is selected from the Italian catalogue;
- the three catalogues (CCI1996, ALPOR and NEIC) are thus merged together, considering as records of the same event those records which differ by less than 1 min in time and less than 0.5° in the epicentral coordinates. The information provided by ALPOR and NEIC is considered only for the events which have no corresponding records in CCI1996.

The updating of UCI2001 is made using the NEIC Preliminary Determinations of Epicentres since 1986. In fact, the NEIC catalogue, analysed for the entire Italian area, appears to satisfy the general conditions required for the routine monitoring of seismicity, since it can be considered complete for magnitudes greater than 3.0, at least after 1985, and it is updated rapidly enough to allow for real-time predictions. A comparative analysis of the catalogues CCI1996 and NEIC permitted to determine the method of merging them together in order to obtain a rather homogenous catalogue that covers the territory of Italy (Peresan and Rotwain, 1998).

The catalogue UCI2001 consists therefore of the following two main parts, covering consecutive time intervals:

– CCI1996 catalogue, 1000–1985, integrated with the ALPOR and NEIC data according to Costa et al. (1996). Events from the CCI1996 are characterised by three magnitude estimations: the local magnitude M_L, the duration magnitude M_d and the magnitude calculated from intensities M_I. For a limited number of relatively large events (M>4.5) the magnitude m_b from ISC bulletins is provided as well. The events from ALPOR or NEIC instead, have their magnitudes assigned according to the priority $M_{ALPOR}(M_L,M_I)$ and $M_{NEIC}(M_L,M_S,m_b)$, respectively.
- NEIC Preliminary Determinations of Epicentres (PDE), since 1986. This part of the catalogue may include up to four magnitude estimations for each event: the surface waves magnitude (M_S) and the body waves magnitude (m_b), both computed by NEIC, plus two values M_1 and M_2, which correspond to magnitudes of a different kind contributed by different agencies (mainly M_L and M_d in the Italian area).

As a consequence, the catalogue UCI2001 contains quite heterogenous estimations of magnitudes, which correspond to M_I and M_L from its beginning up to 1980, and are mainly M_L and M_d after 1981. Since there is no single magnitude scale in UCI2001 which covers the entire time considered, it is necessary to define a combined magnitude scale, before performing any analysis of the seismic flow. The algorithms CN and M8S use the same catalogue UCI2001; the only difference is in the way the operating magnitude is selected for the two algorithms. The M8S algorithm uses the maximum reported magnitude, M_{max}, whereas CN algorithm uses the determination of magnitude selected according to a given priority rule (priority magnitude, $M_{priority}$).

When the priority magnitude is used it is necessary to determine the relationship between each of the magnitudes reported by CCI1996 and by NEIC (Peresan and Rotwain, 1998), in order to preserve the homogeneity of the magnitude estimation. Specifically, for CN application the following priority is considered during the period 1900–1985: M_L, M_d, M_I. In fact M_L is the instrumental magnitude which is reported in the Italian catalogue for the longest interval of time, followed by M_d, which is given starting only in 1980. The magnitude from intensities, M_I, is considered only when no M_L or M_d is provided,

while m_b from ISC is not used at all, since it is given just for a few events and for a limited period of time. Since 1986, i.e. for the period when the NEIC data are used, a suitable choice of priority for magnitudes appears to be: M_2,M_1,M_S, which permits to preserve some homogeneity of the operating magnitude with respect to the CCI1996 catalogue (Peresan and Rotwain, 1998). In this way, priority is given to the magnitude estimations contributed to NEIC by different agencies, that, for the Italian area, correspond mainly to M_d and M_L (M_L are about 10 times more frequent than M_d); as shown by Peresan and Rotwain (1998), both M_1 and M_2 estimates appear quite homogeneous with M_L estimates contained in the CCI1996 catalogue.

The operating magnitudes, M_{max} and $M_{priority}$, for the strong events to be predicted by M8S and CN algorithms are compared in Table 8 (as on May 1, 2004).

Table 8
Operating magnitudes for CN and M8S target events

Time	M_{max}	$M_{priority}$
May 20, 1957	5.8	5.8[a]
August 21, 1962	6.3	5.8[a]
August 21, 1962	6.5	6.0[a]
January 16, 1975	5.5[b]	4.7
May 06, 1976	6.5[b]	6.5[a]
April 15, 1978	5.8[b]	5.5
September 19, 1979	5.8[b]	5.5
May 28, 1980	5.5[b]	5.1
November 23, 1980	6.7[b]	6.5[a]
November 25, 1986	5.5[b]	5.5
February 01, 1988	5.4	5.4[a]
May 05, 1990	5.6[b]	5.5
November 27, 1990	5.6[b]	5.6
February 26, 1991	5.5[b]	5.5
January 05, 1994	5.8[b]	5.4
October 15, 1996	5.8[b]	5.4
September 26, 1997	5.9[b]	5.7[a]
September 26, 1997	6.4[b]	6.0[a]
April 12, 1998	6.0[b]	6.0[b]
May 18, 1998	5.6[b]	5.4
September 09, 1998	5.9[b]	5.7[a]
July 17, 2001	5.5[b]	4.7
September 06, 2002	5.9[b]	5.9
October 31, 2002	5.9[b]	5.7
March 29, 2003	5.5[b]	5.4
September 14, 2003	5.6[b]	5.5[a]
February 23, 2004	5.5[b]	5.3

[a] Target events for CN algorithm.
[b] Target events for M8S algorithm.

Appendix C. Space heterogeneity of catalogues and deep earthquakes

The results of M8S tests in Italy, in the magnitude ranges defined by M6.5+, M6.0+ and M5.5+ (described in Section 4), show that both the strong earthquakes are predicted in the M6.5+ test, while in the M6.0+ test, one earthquake is predicted and the other is missed. In the M5.5+ test, 9 out of 14 earthquakes are predicted. The cases of missed earthquakes raise two important questions. The first one is the well-known problem of the space heterogeneity of the local catalogue data over the territory of Italy and especially near its boundaries, where it is substantially incomplete. The problem has been partly resolved with the UCI2001 catalogue (Peresan and Panza, 2002), integrating the regional catalogue CCI1996 with the ALPOR and NEIC data. Nevertheless, the presence of the two Croatian earthquakes among the failures-to-predict implies further search for the improvement of the catalogue homogeneity, for example, by taking into consideration the Croatian seismic data and by the compilation of a joint, more complete, earthquake catalogue. Such a catalogue will allow the application of M8S algorithm to the region of the entire Adriatic plate and hence the additional testing of the new method on a new set of independent data. At the same time, it will be possible to attempt the application of CN to the same area.

Concerning the algorithm CN, Peresan and Rotwain (1998) showed that the completeness of the NEIC catalogue in the Southern part of Italy is still rather low (about M=3.5 since 1992), and this increases the possibility of failures to predict in the Southern region (Peresan et al., 1999b). This consideration seems supported by the failure to predict, within this area of investigation, of the Pollino earthquake, which occurred in September 9, 1998; the same event, instead, was successfully predicted in the framework of the Central region. Similar arguments also apply to M8S predictions for Southern Italy, where the limited completeness of the catalogue may increase the possibility of failures to predict as well.

The second question concerns the deep earthquakes. The algorithm CN (Keilis-Borok and Rotwain, 1990) usually ignores deep events. On the other side, the standard application of M8 algorithm as in

the global test (Healy et al., 1992; Kossobokov et al., 1997), which aims at the prediction of earthquakes of magnitude M8.0+ or M7.5+, uses the catalogue of main shocks without differentiation of depths. Generally deep earthquakes of such big magnitude are very infrequent and, in many cases, are automatically ignored as the prediction target due to the absence of MS estimate. Besides that, in many regions, deep earthquakes contribute little to the values of M8 functions, since they are a minority of the total population of earthquakes, which is dominated by the shallow ones. When we decrease M_0, the situation changes. Many deep earthquakes become the target of prediction. In the present experiment for M_0=5.5, three large events have depth larger than 100 km. Two of them are missed by M8S, while the third one is predicted. However, in the same area of alarm, a large shallow earthquake, with magnitude 5.9, followed the predicted one with the delay of 4 months. Therefore, the alarm might be caused either by preparation of the two or just the shallow one. Because of that, an experiment similar to what is described here has been performed using the catalogue of the shallow earthquakes only. The elimination of the deep earthquakes from the catalogue UCI2001 affects Southern Italy only and determines a significant reduction of the rate of seismic activity there. This makes it necessary to use lower magnitude thresholds, that is hardly possible due to the limits of the catalogue completeness. Obviously, this affects mainly the M5.5+ application due to the least size of the investigation area. Whereas the results for M6.5+ and M6.0+ are slightly improved: the alarm volume is decreased by a few percents with the retention of the predicted event number. Therefore, to carry on the joint experiment for three consequent magnitude ranges, it has been decided to keep the application of the M8S algorithm using the catalogue of all depth earthquakes, as currently accepted for M8 global applications.

References

Allen, C.R. (Chairman), Edwards, W., Hall, W.J., Knopoff, L., Raleigh, C.B., Savit, C.H., Toksoz, M.N., Turner, R.H. 1976. Predicting earthquakes: a scientific and technical evaluation—with implications for society. Panel on Earthquake Prediction of the Committee on Seismology, Assembly of Mathematical and Physical Sciences. National Research Council, U.S. National Academy of Sciences, Washington, DC.

ALPOR, F.R., 1987. Catalogue of the Eastern Alps. Osservatorio Geofisico Sperimentale, Trieste, Italy. (computer file).

Bak, P., Christensen, K., Danon, L., Scanlon, T., 2002. Unified scaling law for earthquakes. Phys. Rev. Lett. 88, 178501–178504.

Bakun, W.H., Lindh, A.G., 1985. The Parkfield, California, earthquake prediction experiment. Science 229, 619–624.

Boschi, E., Ferrari, G., Gasperini, P., Guidoboni, E., Smiriglio, G., Valensise, G., 1995a. Catalogo dei Forti Terremoti in Italia dal 461 a. C. al 1980. Istituto Nazionale di Geofisica—ING e Storia-Geofisica Ambiente—SGA.

Boschi, E., Gasperini, P., Mulargia, F., 1995b. Forecasting where lager crustal earthquakes are likely to occur in Italy in the near future. Bull. Seismol. Soc. Am. 85 (5), 1475–1482.

Bowman, D.D., Oullion, G., Sammis, C.G., Sornette, A., Sornette, D., 1998. An observational test of the critical earthquake concept. J. Geophys. Res. 103, 24359–24372.

Caputo, M., 1983. The occurrence of large earthquakes in Southern Italy. Tectonophysics 99, 73–83.

Caputo, M., 1988. The forecast of the magnitude 5.8 May 7th 1984 earthquake in Central Italy. Rev. Geofis. 28, 101–121.

Caputo, M., 2000. Comparison of five independent catalogues of earthquakes of a seismic region. Geophys. J. Int. 143, 417–426.

Caputo, M., Gasperini, P., Kelis-Borok, V., Marcelli, L., Rotwain, I., 1977. Earthquake's swarms as forerunners of strong earthquakes in Italy. Ann. Geofis. 30 (3–4), 269–283.

Caputo, M., Console, R., Gabrielov, A.M., Keilis-Borok, V.I., Sidorenko, T.V., 1983. Long-term premonitory seismicity patterns in Italy. Geophys. J. R. Astron. Soc. 75, 71–75. (Roma).

CAT-i Service, 2000. Natural Hazards—Review of the Year 1999. Guy Carpenter and Company. (available for download at www.guycarp.com).

Corral, A., 2003. Local distributions and rate fluctuations in a unified scaling law for earthquakes. Phys. Rev. E, 68:035102 (R) (4 pp.).

Correig, A.M. (Ed.), 2003. Terratrémols i Temporals de Llevant: Dos Exemples de Sistemes Complexos. Jornades Científiques de l'Institut d'Estudis Catalans, Secció de Ciències i Tecnologia (Sèrie Jornades Científiques: 15). Institut d'Estudis Catalans (IEC), Barcelona, 194 pages.

Costa, G., Panza, G.F., Rotwain, I.M., 1995. Stability of premonitory seismicity pattern and intermediate-term earthquake prediction in central Italy. Pure Appl. Geophys. 145 (2), 259–275.

Costa, G., Stanishkova, I.O., Panza, G.F., Rotwain, I.M., 1996. Seismotectonic models and CN algorithm: the case of Italy. Pure Appl. Geophys. 147 (1), 1–12.

Dobrovolsky, I.R., Zubkov, S.I., Miachkin, V.I., 1979. Estimation of the size of earthquake preparation zones. Pure Appl. Geophys. 117, 1025–1044.

Gabrielov, A.M., Dmitrieva, O.E., Keilis-Borok, V.I., Kossobokov, V.G., Kutznetsov, I.V., Levshina, T.A., Mirzoev, K.M., Molchan, G.M., Negmatullaev, S.Kh., Pisarenko, V.F., Prozorov, A.G., Rinheart, W., Rotwain, I.M., Shelbalin, P.N., Shnirman,

M.G., Schreider, S.Yu, 1986. Algorithms of long-term earthquakes' prediction. International School for Research Oriented to Earthquake Prediction–Algorithms. Software and Data Handling, Lima, Perú.

Gabrielov, A.M., Keilis-Borok, V.I., Zaliapin, I.V., Newman, W.I., 2000. Critical transitions in colliding cascades. Phys. Rev., E 62, 237–249.

Gelfand, I., Guberman, Sh., Keilis-Borok, V., Knopoff, L., Press, F., Rantsman, E., Rotwain, I., Sadovsky, A., 1976. Pattern recognition applied to earthquake epicentres in California. Phys. Earth Planet. Inter. 11, 227–283.

Geller, R.J., Jackson, D.D., Kagan, Y.Y., Mulagria, F., 1997. Earthquakes cannot be predicted. Science 275, 1616–1617.

Global Hypocenter Data Base (GHDB), 1989. Global Hypocenter Data Base CD-ROM NEIC/USGS, Denver, CO, 1989 and its updates through January 2002.

Grandori, G., Guagenti, E., Perotti, F., 1988. Alarm systems based on a pair of short-term earthquake precursors. Bull. Seismol. Soc. Am. 78, 1538–1549.

Gusev, A., 1998. Earthquake precursors: banished forever? EOS Trans., AGU 79 (6), 71.

Gutenberg, B., Richter, C.F., 1956. The energy of earthquakes. Q. J. Geol. Soc. Lond. 112, 1–14.

Healy, J.H., Kossobokov, V.G., Dewey, J.W., 1992. A test to evaluate the earthquake prediction algorithm, M8. U.S. Geol. Surv. Open-File Rep. 401, 23 pp.

Jones, L., 1985. Foreshocks and time-dependent earthquake hazard assessment in Southern California. Bull. Seismol. Soc. Am. 75, 1669–1679.

Keilis-Borok, V.I., 1990. The lithosphere of the Earth as a nonlinear system with implications for earthquake prediction. Rev. Geophys. 28, 19–34.

Keilis-Borok, V.I., 1996. Intermediate term earthquake prediction. Proc. Natl. Acad. Sci. U. S. A. 93, 3748–3755.

Keilis-Borok, V.I., Kossobokov, V.G., 1984. A complex of long-term precursors for the strongest earthquakes of the world. Proc. 27th Geological Congress vol. 61. Nauka, Moscow, pp. 56–66.

Keilis-Borok, V.I., Kossobokov, V.G., 1987. Periods of high probability of occurrence of the world's strongest earthquakes. Computational Seismology vol. 19. Allerton Press, pp. 45–53.

Keilis-Borok, V.I., Kossobokov, V.G., 1990. Preliminary activation of seismic flow: algorithms M8. Phys. Earth Planet. Inter. 61, 73–83.

Keilis-Borok, V.I., Rotwain, I.M., 1990. Diagnosis of time of increased probability of strong earthquakes in different regions of the world: algorithm CN. Phys. Earth Planet. Inter. 61, 57–72.

Keilis-Borok, V.I., Soloviev, A. (Eds.), 2003. Nonlinear Dynamics of the Lithosphere and Earthquake Prediction. Springer-Verlag, Berlin-Heidelberg.

Keilis-Borok, V.I., Knopoff, L., Rotwain, I.M., 1980. Burst of aftershocks, long-term precursors of strong earthquakes. Nature 283 (5744), 259–263.

Keilis-Borok, V.I., Kutznetsov, I.V., Panza, G.F., Rotwain, I.M., Costa, G., 1990. On intermediate-term earthquake prediction in Central Italy. Pure Appl. Geophys. 134, 79–92.

Keylis-Borok, V.I., Malinovskaya, L.N., 1964. One regularity in the occurrence of strong earthquakes. J. Geophys. Res. 69, 3019–3024.

Kossobokov, V.G., 1986. The test of algorithm M8. In: Sadovsky, M.A. (Ed.), Algorithms of Long-Term Earthquake Prediction. CERESIS, Lima, Peru, pp. 42–52.

Kossobokov, V.G., 1997. User manual for M8. In: Healy, J.H., Keilis-Borok, V.I., Lee, W.H.K. (Eds.), Algorithms for Earthquake Statistics and Prediction, IASPEI Software Library vol. 6. Seismol. Soc. Am., El Cerrito, CA.

Kossobokov, V.G., Mazhkenov, S.A., 1994. On similarity in the spatial distribution of seismicity. In: Chowdhury, D.K. (Ed.), Computational Seismology and Geodynamics. Am. Geophys. Un. vol. 1. The Union, Washington, DC, pp. 6–15.

Kossobokov, V.G., Healy, J.H., Dewey, J.W., 1997. Testing an earthquake prediction algorithm. Pure Appl. Geophys. 149, 219–232.

Kossobokov, V.G., Maeda, K., Uyeda, S., 1999a. Precursory activation of seismicity in advance of the Kobe, 1995 earthquake. Pure Appl. Geophys. 155, 409–423.

Kossobokov, V.G., Romashkova, L.L., Keilis-Borok, V.I., Healy, J.H., 1999b. Testing earthquake prediction algorithms: statistically significant advance prediction of the largest earthquakes in the Circum-Pacific, 1992–1997. Phys. Earth Planet. Inter. 111, 187–196.

Kossobokov, V.G., Romashkova, L.L., Panza, G.F., Peresan, A., 2002. Stabilizing intermediate-term middle-range earthquake predictions. J. Seismol. Earthq. Eng. 8, 11–19.

Mantovani, E., Albarello, D., 1997. Middle-term precursors of strong earthquakes in southern Italy. Phys. Earth Planet. Inter. 101, 49–60.

Martinelli, G., 2000. Contributions to a history of earthquake prediction research. Seismol. Res. Lett. 71 (5), 583–588.

Meletti, C., Patacca, E., Scandone, P., 2000. Construction of a seismotectonic model: the case of Italy. Pure Appl. Geophys. 157, 11–35.

Minster, J.B., Williams, N.P., 1992. The "M8" intermediate term earthquake prediction algorithm: an independent assessment. EOS Transactions 73 (43), 366. (AGU Fall Meeting).

Minster, J.B., Williams, N.P., 1996. Intermediate term earthquake prediction algorithms. Southern California Earthquake Center, Progress Report, November 1996, 491–496.

Molchan, G.M., 1990. Strategies in strong earthquake prediction. Phys. Earth Planet. Inter. 61, 84–98.

Molchan, G.M., 1996. Earthquake prediction as a decision-making problem. Pure Appl. Geophys. 147 (1), 1–15.

Molchan, G.M., Dmitrieva, O.E., 1992. Aftershocks identification: methods and new approaches. Geophys. J. Int. 190, 501–516.

Molchan, G.M., Dmitrieva, O.E., Rotwain, I.M., Dewey, J., 1990. Statistical analysis of the results of earthquake prediction, based on burst of aftershocks. Phys. Earth Planet. Inter. 61, 128–139.

Molchan, G.M., Kronrod, T.L., Panza, G.F., 1997. Multiscale seismicity model for seismic risk. Bull. Seismol. Soc. Am. 87 (5), 1220–1229.

Nature Debates, 1999. http://www.nature.com/nature/debates/earthquake/equake_frameset.html.
National Earthquake Information Centre (NEIC), 1990. Earthquake Hypocenters Data Files. USGS, USA, and their updates (Preliminary Determinations of Epicentres, PDE, and Quick Epicentral Determinations, QED). Ftp site: ghtftp.cr.usgs.gov.
Peresan, A., Panza, G.F., 2002. UCI2001: The updated catalogue of Italy, ICTP, Trieste, Italy, Internal report IC/IR/2002/3.
Peresan, A., Rotwain, I.M., 1998. Analysis and definition of magnitude selection criteria for NEIC (PDE) data, oriented to the compilation of a homogenous updated catalogue for CN monitoring in Italy. The Abdus Salam International Centre for Theoretical Physics, ICTP. Internal report. Trieste. Italy. IC/98/97.
Peresan, A., Costa, G., Vaccari, F., 1997. CCI1996: the Current Catalogue of Italy. The Abdus Salam International Centre for Theoretical Physics, ICTP. Internal report. Internal report IC/IR/97/9, Trieste, Italy.
Peresan, A., Costa, G., Panza, G.F., 1999a. Seismotectonic model and CN earthquake prediction in Italy. Pure Appl. Geophys. 154, 281–306.
Peresan, A., Costa, G., Panza, G.F., 1999b. A proposal of regionalization for the application of the CN earthquake prediction algorithm to the Italian territory. Ann. Geofis. 42, 281–306.
Peresan, A., Panza, G.F., Costa, G., 2000. CN algorithm and long lasting changes in reported magnitudes: the case of Italy. Geophys. J. Int. 141, 425–437.
Peresan, A., Rotwain, I., Zaliapin, I., Panza, G.F., 2002. Stability of intermediate-term earthquake predictions with respect to random errors in magnitude: the case of Central Italy. Phys. Earth Planet. Inter. 130, 117–127.
Postpischl, D., 1985. Catalogo dei terremoti dall'anno 1000 al 1980. C.N.R.-Progetto Finalizzato Geodinamica.
Richter, C.F., 1964. Discussion of paper by V.I. Keylis-Borok and L.N. Malinovskaya, 'One regularity in the occurrence of strong earthquakes'. J. Geophys. Res. 69, 3025.
Romashkova, L.L., Kossobokov, V.G., 1996. Source concentration parameters in an intermediate-term earthquake prediction algorithm. In: Keilis-Borok, V.I., Molchan, G.M. (Eds.), Modern Problems of Seismology and Earth Dynamics. Comput. Seismol. vol. 28. Nauka, Moscow, pp. 56–66 (in Russian).
Romashkova, L.L., Kossobokov, V.G., Panza, G.F., Costa, G., 1998. Intermediate-term prediction of earthquakes in Italy: algorithm M8. Pure Appl. Geophys. 152, 37–55.
Rotwain, I.M., Novikova, O., 1999. Performance of the earthquake prediction algorithm CN in 22 regions of the world. Phys. Earth Planet. Inter. 111, 207–213.
Sadovsky, M.A. (Ed.), Long-Term Earthquake Prediction: Methodological Recommendations. Publication of Ac.Sc. USSR-Inst. Phys. Earth, Moscow. 127 pp. (in Russian).
Scandone, P., Patacca, E., Meletti, C., Bellatalla, M., Perilli, N., Santini, U., 1990. Struttura geologica, evoluzione cinematica e schema sismotettonico della penisola italiana. Atti Conv. GNDT 1, 119–135. (in Italian).
Shebalin, P.N., 1992. Automatic duplicate identification in set of earthquake catalogues merged together. Open-File Rep. U.S. Geol. Surv., 92–401 (Appendix II).
Updike, R.G. (Ed.), Proceedings of the National Earthquake Prediction Evaluation Council, Open-File Rep. U.S. Geol. Surv., pp. 89–114.
Wells, D.L., Coppersmith, K.J., 1994. New empirical relationships among magnitude, rupture length, rupture width, rupture area, and surface displacement. Bull. Seismol. Soc. Am. 84, 974–1002.
Wyss, M. (Ed.), 1991. Evaluation of Proposed Earthquake Precursors. AGU, Washington, DC.
Wyss, M., 1997a. Cannot earthquakes be predicted? Science 278, 487–488.
Wyss, M., 1997b. Second round of evaluation of proposed earthquake precursors. Pure Appl. Geophys. 149, 3–16.
Zuniga, F.R., Wyss, M., 1995. Inadvertent changes in magnitude reported in earthquake catalogs: their evaluations through the b-value estimates. Bull. Seismol. Soc. Am. 5, 1858–1866.

Antonella Peresan, PostDoc at the Department of Earth Sciences, University of Trieste. She received her PhD in geophysics, in 2000, and her laurea in physics, in 1996, from the University of Trieste. She is an active member of the International Centre for Theoretical Physics—SAND Group since 1998. Her research activities concern the analysis of seismicity patterns in tectonic and volcanic areas and in synthetic seismicity, involving testing and application of intermediate-term earthquake prediction algorithms and their integration with the procedures for deterministic hazard assessment, as well as the numerical block structure simulation of the lithosphere dynamics.

Vladimir G. Kossobokov. Leading researcher at the International Institute of Earthquake Prediction Theory and Mathematical Geophysics—Russian Academy of Sciences, Moscow. MS in Mathematics, Department of Mechanics and Mathematics, Moscow State University (1975); PhD in Geophysics at the Institute of Physics of the Earth, USSR Academy of Sciences, Moscow (1984). Since 1999 an expert of European Advisory Evaluation Committee for Earthquake Prediction, Council of Europe. One of the authors of reproducible earthquake prediction algorithms and their on-going global real-time testing aimed at the largest earthquakes worldwide. He suggested a generalization of the fundamental Gutenberg–Richter scaling law, which takes into account the fractal properties of earthquake distribution.

Leontina L. Romashkova, Research fellow of the International Institute of Earthquake Prediction Theory and Mathematical Geophysics, Russian Academy of Sciences, Moscow. MSc in Applied Mathematics and Physics from Moscow Institute of Physics and Technology in 1990, visiting researcher of ICTP, SAND Group since 1996. Scientific contributions: Development and application of reproducible intermediate-term earthquake prediction algorithms, aimed at the prediction of large earthquakes in regions all over the world, and investigation of seismic dynamics prior to and after the largest earthquakes worldwide.

Giuliano F. Panza, Professor of seismology in the Department of Earth Sciences—University of Trieste, and head of SAND Group ICTP-Trieste. Laurea in physics from the University of Bologna in 1967; PostDoc at UCLA. He is a fellow of Academia Nazionale dei Lincei, of Academia Europea, and Third World Academy of Sciences. He is foreign member of the Russian Academy of Sciences. He is a winner of the EGS Beno Gutermberg medal in 2000, and received Laurea Honoris Causa in Physics in 2002 from the University of Bucharest. He is the leader of several projects funded by EC related to seismic hazard assessment.